Mattia Storti[1], Anna Segalla[1], Marco Mellon[1], Alessandro Alboresi[1] and Tomas Morosinotto[1]

Department of Biology, University of Padova, 35121 Padova, Italy

Corresponding author: Tomas Morosinotto, Dipartimento di Biologia, Università di Padova, Via Ugo Bassi 58B, 35121 Padova, Italy. Tel. +390498277484, Email: tomas.morosinotto@unipd.it

Regulation of electron transport is essential for photosystem I stability and plant growth

Short tile: Regulation of photosynthesis is essential

The author(s) responsible for distribution of materials integral to the findings presented in this article in accordance with the policy described in the Instructions for Authors (www.plantcell.org) is Tomas Morosinotto, tomas.morosinotto@unipd.it

Abstract

Life depends on the ability of photosynthetic organisms to exploit sunlight to fix carbon dioxide into biomass. Photosynthesis is modulated by pathways such as cyclic and pseudocyclic electron flow (CEF and PCEF). CEF transfers electrons from photosystem I to the plastoquinone pool according to two mechanisms, one dependent on proton gradient regulators (PGR5/PGRL1) and the other on the type I NADH dehydrogenase (NDH) complex. PCEF uses electrons from photosystem I to reduce oxygen; in several groups of photosynthetic organisms but not in angiosperms, it is sustained by flavodiiron proteins (FLVs). PGR5/PGRL1, NDH and FLVs are all active in the moss *Physcomitrella patens,* and mutants depleted in these proteins show phenotypes under specific light regimes. Here, we demonstrated that CEF and PCEF exhibit strong functional overlap and that when one protein component is depleted, the others can compensate for most of the missing activity. When multiple mechanisms are simultaneously inactivated, however, plants show damage to photosystem I and strong growth reduction, demonstrating that mechanisms for the modulation of photosynthetic electron transport are indispensable.

Introduction

Oxygenic photosynthesis enables plants, algae and cyanobacteria to exploit light to fix carbon dioxide, directly or indirectly supporting the metabolism of most living organisms. In photosynthetic organisms, sunlight powers the linear electron flow (LEF) from water to $NADP^+$ via the activity of two photosystems (PS), PSII and PSI, generating NADPH and ATP to sustain cellular metabolism. Natural environmental conditions are highly variable, and sudden changes in irradiation can drastically affect the flow of excitation energy and electrons. The ATP and NADPH consumption rate is also highly dynamic because of continuous metabolic regulation (Kulheim et al., 2002; Allahverdiyeva et al., 2015; Peltier et al., 2010). Photosynthetic organisms have indeed evolved multiple mechanisms to modulate the flow of excitation energy and electrons according to metabolic constraints and environmental cues, for instance, by diverting/feeding electrons from/to the linear transport chain. These mechanisms include the cyclic electron flow (CEF) around PSI, in which electrons are transferred from photosystem I back to the plastoquinone pool, contributing to proton translocation and ATP synthesis but not to NADPH formation (Shikanai, 2014; Joliot and Johnson, 2011; Arnon and Chain, 1975; Shikanai and Yamamoto, 2017). Two distinct CEF pathways have been identified, although the precise molecular mechanisms of the electron transport reactions involved are still under debate (Nawrocki et al., 2019); one of these pathways is dependent on a chloroplast NDH complex (Shikanai et al., 1998) and the other on PGR5/PGRL1

(Munekage et al., 2002; DalCorso et al., 2008; Hertle et al., 2013). Another alterative electron pathway is the pseudocyclic electron flow (PCEF), in which electrons from PSI are used to reduce oxygen (O_2) to water. PCEF is also known as the water-to-water cycle because H_2O is split by PSII and then resynthesized when O_2 replaces $NADP^+$ as the final electron acceptor downstream of PSI. PCEF includes the Mehler reaction, which is important for detoxifying $O_2^{\cdot-}$ produced by PSI (Asada, 2000) but is estimated to make a limited contribution to electron transport (Driever and Baker, 2011). More recently, enzymes known as flavodiiron proteins (FLVs or FDPs) have been shown to contribute to PCEF (Allahverdiyeva et al., 2013), which is also responsible for significant transient electron transport in *Physcomitrella patens* (Gerotto et al., 2016).

CEF and PCEF activities are found in all organisms that perform oxygenic photosynthesis, but the molecular machineries involved are not fully conserved and differ in various phylogenetic groups (Alboresi et al., 2019). In different species of cyanobacteria, unicellular eukaryotic algae and plants, the analysis of specific mutants has clearly shown that mechanisms for the regulation of photosynthetic electron transport play a key role in the response to dynamic environmental conditions (Suorsa et al., 2012; Yamori and Shikanai, 2016; Shikanai and Yamamoto, 2017). For example, FLV was shown to play an important role in the response to fluctuating light in different organisms (Gerotto et al., 2016; Chaux et al., 2017; Allahverdiyeva et al., 2013), while PGRL1/PGR5 have important functions under saturating or fluctuating light and anoxia (Kukuczka et al., 2014; Munekage et al., 2002; Suorsa et al., 2012). The inactivation of NDH alone has no major impact on growth and stress responses (Endo et al., 1999; Ishikawa et al., 2008; Yamori et al., 2015), although its activity seems to be essential for C4 metabolism (Ishikawa et al., 2016).

In the present work, we generated mutants defective in CEF and PCEF mechanisms by simultaneously knocking out *pgrl1*, *ndhm* and *flva* in the moss *Physcomitrella patens*. The results demonstrate strong functional overlap, as when one protein was depleted, its activity was largely compensated by the others. However, plants with multiple deletions showed very severe phenotypes, demonstrating that the regulation of electron transport is indispensable for PSI stability and growth in any environmental condition.

Results

CEF and PCEF mechanisms are fundamental for photosynthetic activity

In *P. patens* plants depleted of FLVA, PGRL1, and NDHM, mechanisms for the regulation of photosynthetic electron transport are affected (Storti et al., 2019; Gerotto et al., 2016; Kukuczka et al., 2014).These plants were used to generate all combinations of double mutants (*flva-pgrl1*, *flva-ndhm*, *pgrl1-ndhm)* as well as triple *flva-pgrl1-ndhm* KO plants depleted in all three mechanisms in

the present study. In all cases, multiple independent lines for each genotype were validated for the correct insertion of the resistance cassette at the desired *loci* as well as for the absence of the expression of the corresponding gene. Moreover, triple mutant lines were generated starting from two distinct double-mutant lines (i.e., either *flva-ndhm* or *flva-pgrl1*) to further ensure that the observed plant phenotypes were not due to secondary effects in the selected genetic background (Figure S1).

Western blotting analysis of proteins of the photosynthetic apparatus confirmed the absence of target proteins such as FLVA and NDHM (Figure 1). FLVB was also strongly reduced in the absence of FLVA, as expected considering their heteromeric assembly (Gerotto et al., 2016). FLVA and FLVB were significantly reduced upon *pgrl1-ndhm* KO as well. No specific antibody was available for PGRL1, but its absence was verified by mass spectrometry in the parental lines (Kukuczka et al., 2014). Among the other components of the photosynthetic apparatus, PSI content was reduced, while the relative contents of ATPase, CP47 and PSBS increased in the *flva-pgrl1-ndhm* KO plants. Native PAGE analysis confirmed a clear reduction in PSI-LHCI content in *pgrl1-ndhm* KO plants and especially in the triple *flva-pgrl1-ndhm* KO plants (Figure 2B). This was confirmed by the spectroscopic evaluation of the PSI/PSII ratio (Figure 2C), which showed a strong relative reduction in active PSI upon *pgrl1-ndhm* and *flva-pgrl1-ndhm* KO. The pigment content was highly similar among the lines, with only a slight decrease in the Chl a/b content under *flva-pgrl1-ndhm* KO, consistent with a lower PSI content (Table S2).

The measurement of photosynthetic electron transport (ETR) in WT plants showed a first peak a few seconds after the light was switched on, largely due to FLV activity (Gerotto et al., 2016), which was consistently absent in all *flva*-less plants (Figure 2A-B). This first peak reduced in *pgrl1-ndhm* KO plants but not in the corresponding single KO mutants (Figure S2). This finding supports the hypothesis that CEF can contribute to the activation of electron transport upon dark-to-light transition, even though the reduced FLV accumulation observed in *pgrl1-ndhm* KO plants (Figure 1A) can explain this observation.

On longer timescales, ETR increases slowly following the activation of carbon fixation, reaching a steady state after ≈ 3 minutes. In all double mutants (*flva-pgrl1*, *flva-ndhm*, *pgrl1-ndhm* KO), steady-state ETR was indistinguishable from that in the WT (Figure 2A-B). These mutants also exhibited an equivalent capacity to generate a proton motive force across the thylakoid membranes (Figure 2C), oxygen evolution activity (Figure 2D-E) and photosystem II yield (Figure 2F), showing that all double-mutant plants can sustain the same photosynthetic activity as WT plants under stationary conditions. The picture is completely different in triple *flva-pgrl1-ndhm* KO plants, in which the ETR capacity is greatly reduced even under steady-state photosynthesis after several

minutes of illumination (Figure 2B). The proton motive force and oxygen evolution are also affected, showing that simultaneous depletion of CEF and PCEF has a drastic impact on photosynthetic activity (Figure 2C-D).

CEF activity in *P. patens* is pronounced only in the first few seconds after light is switched on, while it is very low in a steady state (Kukuczka et al., 2014). Dark-adapted *flv* KO plants showed sustained CEF in the first seconds of illumination compared to WT (Gerotto et al., 2016). Here, DCMU-treated samples of *pgrl1-ndhm* and *flva-pgrl1-ndhm* KO plants showed reduced CEF compared to *flva-pgl1* and *flva-ndhm* KO plants, supporting the idea that PGRL1 and NDH are responsible for CEF in *P. patens* (Figure S3).

In WT plants exposed to saturating illumination, PSI activity is limited on the donor side (Figure 2H), while in *flva-pgrl1-ndhm* KO plants, PSI activity is always limited from the acceptor side (Figure 2G-H). In *flva-pgrl1-ndhm* triple KO, PSI and PSII are saturated even under dim illumination (Figure 2G, Figure S5) and show strong PQ overreduction, suggesting that electron transport is limited by PSI activity (Figure S6). This suggests that the cumulative activity of CEF and PCEF is indispensable even at low light intensities to keep the PSI acceptor side oxidated.

Regulation of photosynthetic electron transport is critical for plant growth in all light conditions

The impact of the mutations on plant growth was assessed by cultivation under different light regimes. All double mutants showed no major defects under non-saturating light (10-50 µmol photons m^{-2} s^{-1}), while differences emerged in more challenging conditions. All plants depleted in PGRL1 showed a growth reduction under strong constant illumination, while all plants depleted in FLVA exhibited less growth when exposed to fluctuating light (FL), as previously reported (Storti et al., 2019; Gerotto et al., 2016). A small growth reduction was also observed in *pgrl1-ndhm* KO plants exposed to light fluctuations, in contrast to both single KO mutants that provided the genetic background (Figure 3, Figure S2). The most striking observation, however, was that *flva-pgrl1-ndhm* triple KO plants showed a 60-75% growth reduction with respect to the WT plants in all conditions, including very low, limiting light (10 µmol photons m^{-2} s^{-1}). In non-saturating illumination, the phenotype of the *flva-pgrl1-ndhm* KO plants was, thus, completely different from those of all the double mutants, highlighting that the mechanisms for the regulation of photosynthetic transport are essential for plant growth.

Such a severe growth phenotype, however, was not present in the rich medium with 0.5% glucose and 0.05% ammonium tartrate used for plant propagation (Figure 4A). The addition of metabolizable sugars such as sucrose or glucose to the basal salt medium was indeed sufficient to restore plant growth to WT levels. Interestingly, photosynthetic functionality in these plants was not

recovered, and PSI/PSII and ETR remained largely depleted (Figure 4C, S8). This suggests that *flva-pgrl1-ndhm* KO mutant growth impairment is due to a reduced energy supply from photosynthesis and can be rescued by providing an external carbon source. This result also demonstrates the ability of *P. patens* to grow well under mixotrophic metabolism with most of the energy provided by organic substrates, which may be related to adaptation to ecological niches with available decomposing biomass.

The impact of several different parameters affecting photosynthetic metabolism was assessed to further investigate the mechanistic reason for the strong impact on growth. Plants were cultivated under saturating CO_2 to stimulate carbon fixation and minimize photorespiration, with 24 hours of continuous non-saturating light to avoid any dark-light transition. As shown in Figure 4B, continuous light and high CO_2 induced a slight increase in growth, but this was similar in mutant and WT plants. The same experiments were repeated with plants cultivated under very low light for several weeks. In this case, we observed a slight recovery of the growth rate and PSI/PSII, suggesting that PSI is indeed light damaged in *flva-pgrl1-ndhm* KO plants and that the recovery is extremely slow (Figure 4C).

Discussion

Mechanisms for alternative electron transport play fundamental biological roles despite their apparent limited electron transport capacity

CEF and PCEF regulate photosynthesis in cyanobacteria, algae and plants, and corresponding mutant lines show phenotypes under specific growth conditions such as saturating or fluctuating light (Allahverdiyeva et al., 2013; Yamori and Shikanai, 2016; Peltier et al., 2016). The analysis of triple *flva-pgrl1-ndhm* KO plants instead showed that the simultaneous depletion of CEF and PCEF drastically affects plant photosynthetic activity even under optimal growth conditions. Accordingly, *Arabidopsis* double mutants lacking both CEF activities (i.e., : *pgr5* and *chlororespiratory reduction/crr* depleted in the NDH complex) show strong growth phenotypes compared to WT (Munekage et al., 2004).

As an angiosperm, *Arabidopsis* lacks FLV, and its CEF is estimated to contribute approx. 10% of total proton motive force (pmf, (Shikanai, 2016; Avenson et al., 2005)), with a larger role in dark-light conditions or specific developmental stages (Joliot et al., 2004; Allorent et al., 2015). In *P. patens*, linear electron transport is estimated to represent over 95% of the total flow under steady-state photosynthesis, with a larger contribution from PCEF and CEF to pmf only being measurable during dark-to-light transitions (Figure 2 and S3) or under peculiar conditions such as anoxia (Kukuczka et al., 2014). These values are estimations of the maximal ETR capacity under saturating

illumination, and the actual contribution of these alternative pathways to pmf under dim light could therefore be even smaller. On the other hand, it should be considered that the estimated contributions of the individual components of CEF and PCEF to electron transport are based on the analysis of single mutants, but the presence of compensation phenomena, as demonstrated here, can lead to the underestimation of the capacity of single routes, making the overall picture more uncertain. Even considering mitigating factors, in both *A. thaliana* and *P. patens*, such a small reduction in the electron transport capacity is expected to have only a slight impact on growth if any and, thus, does not explain the strong phenotype of *Arabidopsis pgr5-crr* mutant plants (Munekage et al., 2004) and *P. patens flva-pgrl1-ndhm* KO plants (Figure 3-4).

All these considerations clearly suggest that the main biological roles of CEF and PCEF are not to enhance but rather to modulate ETR and, in particular, to protect PSI from overreduction and consequent damage (Tiwari et al., 2016). Remarkably, in the triple *flva-pgrl1-ndhm* KO plants PSI is largely photoinactivated even when exposed to highly limiting illumination (10 µmol photons m^{-2} s^{-1}, Figure 1-3). Only with prolonged exposure to a very low light intensity for several weeks was it possible to detect a recovery in PSI activity in *flva-pgrl1-ndhm* KO plants (Figure 4), showing that PSI is highly unstable in these mutants. The extremely slow recovery also indicated that there is not an efficient repair mechanism for PSI, representing a drastic difference from the situation for PSII, which is continuously damaged but also efficiently repaired (Järvi et al., 2015). These data point to a protection strategy in which PSII is the main target of light damage in WT plants and is continuously repaired, while PSI is highly stable (Tikkanen et al., 2014; Larosa et al., 2018). Such a strategy provides an advantage because the damage is only concentrated on one complex and specifically on one protein, the PSII subunit D1 (Järvi et al., 2015), which can be efficiently repaired, while all other protein components have a much longer turnover. Considering that photosystems are large pigment-protein complexes that accumulate at high levels in the chloroplasts, such a strategy would be efficient in saving energy and nutrients. A further factor to be considered is that the synthesis of pigment protein complexes is potentially dangerous for the cells since pigments that are free or bound to partially assembled complexes are strong ROS producers and are easily damaged by illumination. Slowing down the turnover of these complexes and, thus, reducing the number and type of complexes that are continuously assembled may therefore represent an additional advantage.

As shown here, however, such a protection strategy is only effective if PSI is indeed very stable, since any damage to this complex will cause major consequences for growth because of the slow turnover and absence of efficient repair. Hence, PSI needs to be efficiently protected, which is

achieved by the presence of multiple, redundant mechanisms that have evolved to ensure its stability under all environmental conditions, as shown in this work.

Regulation of electron transport adapted during evolution to balance efficiency and photoprotection

Photosynthetic organisms present multiple mechanisms for the regulation of photosynthetic electron transport; in addition to the CEF and PCEF mechanisms discussed herein, mitochondrial respiration and photorespiration also play a significant role. The relative biological relevance of these multiple mechanisms is still debated, and the results presented here demonstrate that the biological activity of CEF and PCEF is likely underestimated from the analysis of single mutants, with the most evident example being the NDH complex. Different plant species depleted in chloroplast NDH activity show no growth effects under any light conditions and present photosynthetic properties close to WT plants (Peltier et al., 2016; Yamori and Shikanai, 2016; Ishikawa et al., 2008). A similar situation is observed in *P. patens* (Figure S2), but the situation is completely different when NDH is depleted from *flva-pgrl1* KO plants, where it causes drastic impairment of photosynthetic activity. A similar phenomenon was found in *A. thaliana* when the *pgr5* and *pgr5-crr* mutants were compared (Munekage et al., 2004). Another even more surprising line of evidence that CEF and PCEF present functional overlap is provided by the demonstration that in angiosperms (both *A. thaliana* and rice), the expression of *P. patens* FLV complements the high-PSI-acceptor-side-limitation phenotype of CEF-depleted plants, protecting the system from photodamage under fluctuating light (Wada et al., 2018; Yamamoto et al., 2016).

This strong functional overlap helps to explain why CEF and PCEF mechanisms are not fully conserved in all photosynthetic organisms despite their major biological role in PSI protection. For example, FLV proteins are present and active in cyanobacteria, green algae, mosses and gymnosperms but have been lost by angiosperms and by some secondary endosymbiotic algae, such as diatoms (Ilík et al., 2017; Bellan et al., 2019; Shimakawa et al., 2018). The most parsimonious hypothesis is that FLVs were present in the prokaryotic cyanobacterial ancestor but were later independently lost at least twice in eukaryotes. Based on the functional complementarity observed here, if one mechanism for the regulation of electron transport is lost, the others are likely capable of compensating for most of the missing activity. Consistent with this idea is the observation that angiosperms are missing FLV, but they rely on CEF to respond to light fluctuations, as shown by the sensitivity of *pgr5/prgl1* KO in *Arabidopsis* to these conditions(Suorsa et al., 2012), which is not observed in *P. patens* (Storti et al., 2019). This is also consistent with the stronger CEF activity in *Arabidopsis* than in *P. patens* (Avenson et al., 2005).

The observation that FLV was lost at least twice during the evolution of photosynthetic organisms suggests that its activity may present some competitive disadvantages. FLV indeed drives energy loss since electrons are donated back to oxygen, generating a futile cycle with water oxidation in PSII. This energy loss is reduced by the regulation of FLV activity, which is maximal only under light fluctuations and is only detectable for a few seconds (Gerotto et al., 2016). Indeed, FLV activity is not detectable during steady-state illumination, and *flv* KO mutants exhibit ETR that is indistinguishable from that in WT plants (Gerotto et al., 2016). However, this conclusion is challenged by the comparison of *pgrl1-ndhm* KO and *flva-pgrl1-ndhm* KO plants, which only differ in the presence of FLV. These plants show a highly different phenotype in low steady illumination, demonstrating that FLV can sustain steady-state photosynthesis even in the absence of light fluctuations (Figure 3). This suggests that in WT plants, FLV could potentially accept electrons from PSI at a low, undetectable rate. Another indication that FLV is potentially constantly active is that the growth of the *pgrl1-ndhm* KO mutant of *P. patens* examined in this study is not as affected as that of the corresponding *Arabidopsis* mutant, while the phenotypes are analogous in *flva-pgrl1-ndhm* KO plants, suggesting that FLV indeed complements the depleted CEF activity *in vivo*. This evidence suggests that, even if it is not measurable when CEF is active, FLV potentially shows constant activity under low limiting illumination, where the use of electrons to reduce oxygen to water represents an energy loss and potentially a disadvantage that could drive FLV loss during evolution.

Considering the impact on PSI protection and growth when FLV is depleted, it can be asked whether FLV introduction in angiosperm crops could potentially lead to increased biomass productivity and yield. While preliminary promising results have been obtained (Wada et al., 2018), some caution is probably necessary. As discussed, it is in fact possible that FLV activity can cause low constant energy loss, and thus, improved productivity would be possible only if this energy loss is compensated by increased PSI photoprotection. According to the present literature, PSI should rarely be damaged in natural conditions, as there are only a few reports of this happening in a few species under specific chilling conditions (Tjus et al., 1998; Terashima et al., 1994). If this is the case and PSI protection mechanisms are indeed very efficient, then the introduction of FLV should have a limited impact. If instead PSI indeed experiences damage, then FLV reintroduction should provide an advantage, at least in some specific conditions.

Methods

Plant material and growth. P. patens (Gransden) wild-type (WT) KO lines were maintained in the protonemal stage by vegetative propagation and grown under controlled conditions: 24°C, 16 h

light/ 8 h dark photoperiod with 50 µmol photons $m^{-2}s^{-1}$ (Control light, CL) unless otherwise specified. Physiological and biochemical experiments were performed on 10-day-old plants grown in $PpNO_3$ medium. Growth in different media and light conditions was evaluated starting from protonema colonies of 2 mm in diameter and then followed for 21 days. Colony size was measured as reported in a previous study (Storti et al., 2019).

Moss transformation and mutant selection. The *pgrl1* (Gerotto et al., 2016; Kukuczka et al., 2014) construct was used to remove the *pgrl1* gene from the *ndhm* single KO genetic background (Storti et al., submitted) to obtain *pgrl1-ndhm* double KO mutants. For triple mutant isolation, the *pgrl1* construct was used to remove *pgrl1* from the *flva-ndhm* background. A similar *ndhm* KO construct (Storti et al., submitted) was used to remove the gene from the *flva-pgrl1* KO background, obtaining triple *flva-pgrl1-ndhm* KO mutant plants in both cases (Figure S1). Transformation was performed via protoplast DNA uptake as described in (Alboresi et al., 2010). After two rounds of selection, the various lines were homogenized using 3 mm zirconium glass beads (Sigma-Aldrich), and genomic DNA (gDNA) was isolated according to a rapid extraction protocol (Edwards et al., 1991) with minor modification. PCR amplification was performed on extracted gDNA (Table S1; Figure S1). RT-PCR was performed on cDNA (RevertAid Reverse Transcriptase, Thermo Scientific) synthetized after RNA extraction(Allen et al., 2006) to confirm the *pgrl1-ndhm* and *flva-pgrl1-ndhm* KO lines.

Spectroscopic analyses. In vivo chlorophyll fluorescence and $P700^+$ absorption were monitored simultaneously at room temperature with a Dual-PAM 100 system (Walz) in protonemal tissue grown for 10 days in $PpNO_3$. Before the measurements, the plants were dark-acclimated for 40 min, and the F_v/F_m parameter was calculated as $(F_m-F_0)/F_m$. To determine the induction curves, actinic red light was set at 50 or 540 µmol photons $m^{-2}s^{-1}$, and photosynthetic parameters were recorded every 30 s. At each step, the photosynthetic parameters were calculated as follows: Y(II) as (Fm'-F0)/Fm', qL as $(F_m'-F)/(F_m'-F_0')$ x F_0'/F and NPQ as $(F_m-F_m')/F_m'$, Y(I) as 1-Y(ND)-Y(NA); Y(NA) as $(P_m-P_m')/P_m$; Y(ND) as (1 - P700 red). Electrochromic shift (ECS) spectra were recorded with a JTS-10 system (Biologic) in plants that were dark adapted and soaked with 20 mM HEPES, pH 7.5. and 10 mM KCl; the 546 nm background was subtracted from the 520 nm signal. Functional photosystem quantification was performed by single flash turnover using a xenon lamp. Samples were infiltrated with 20 µM DCMU and 4 mM HA (hydroxylamine) to eliminate the contribution of PSII. ETR was evaluated by DIRK (dark-induced relaxation kinetic) analysis as in (Gerotto et al., 2016) and normalized to the total PS content (PSI + PSII). After five minutes, the light was switched off for 20 s to follow relaxation kinetics and evaluate the proton motive force

generated during light treatment (Storti et al., 2019). gH^+ was calculated from the half time ($t_{1/2}$) of ECS relaxation in the dark after exposure to five minutes of illumination (940 µmol photons $m^{-2}s^{-1}$).

Western blot analysis. Total protein extracts were obtained by grinding protonemal tissues in solubilization buffer (50 mM TRIS pH 6.8, 100 mM DTT, 2% SDS and 10% glycerol). Samples were loaded so that the same amount of chlorophyll was present, and after SDS-PAGE, proteins were transferred to a nitrocellulose membrane (Pall Corporation). Membranes were hybridized with specific primary antibodies (anti-PsaA, Agrisera, catalog number AS06 172; anti-PsaD, Agrisera, catalog number AS09 461; anti-Cyt f, Agrisera, catalog number AS06 119; anti-γ-ATPase, Agrisera, catalog number AS08 312; custom made anti-FLVA and FLVB (Gerotto et al., 2016), and custom made anti-D2, anti-CP47, anti-PSBS, anti-LHCSR and anti-NDHM) and detected with alkaline phosphatase conjugated antibody (Sigma Aldrich).

Clear native (CN) gel. Gel were casted in 8x10 cm plates using buffer described by (Kügler et al., 1997), running gel was obtain by using an acrylamide gradient of 4-12%, and 4% acrylamide in the stacking. Thylakoids from dark adapted protonemal tissue were isolated as in (Gerotto et al., 2012) and resuspended in 25BTH20G (25mM BisTris-HCl pH 7, 20% glycerol) buffer at 1 µg chl/ µl concentration. Thylakoids were solubilized as described in (Järvi et al., 2011), using 0.75 % α-DM (α -dodecylmaltoside) and adding deoxycholic acid (DOC 0.2%) to solubilized samples. Anode and cathode buffer were the same used by (Järvi et al., 2011) for CN gel, cathode buffer was addicted with 0.05% DOC and 0.02% α -DM. Gel were run for 4h with increasing voltage (75-200 V).

Author contributions.

T.M. and A.A. designed the research. M.S., A.S., M.M, A.A. performed experiments; M.S, A.A and T.M. analyzed the data. T.M. wrote the paper. All authors reviewed the manuscript.

Acknowledgements.

AA acknowledges the financial support by the University of Padova. TM received financial support by the European Research Council (BIOLEAP grant no. 309485).

References.

Alboresi, A., Gerotto, C., Giacometti, G.M., Bassi, R., Morosinotto, T. (2010). Physcomitrella patens mutants affected on heat dissipation clarify the evolution of photoprotection mechanisms upon land colonization. Proc. Natl. Acad. Sci. U. S. A. **107**: 11128–33.

Alboresi, A., Storti, M., and Morosinotto, T. (2019). Balancing protection and efficiency in the regulation of photosynthetic electron transport across plant evolution. New Phytol. **221**: 105–

109.

Allahverdiyeva, Y., Mustila, H., Ermakova, M., Bersanini, L., Richaud, P., Ajlani, G., Battchikova, N., Cournac, L., and Aro, E.-M. (2013). Flavodiiron proteins Flv1 and Flv3 enable cyanobacterial growth and photosynthesis under fluctuating light. Proc. Natl. Acad. Sci. U. S. A. **110**: 4111–6.

Allahverdiyeva, Y., Suorsa, M., Tikkanen, M., and Aro, E.-M.E.-M. (2015). Photoprotection of photosystems in fluctuating light intensities. J. Exp. Bot. **66**: 2427–36.

Allen, G.C., Flores-Vergara, M.A., Krasynanski, S., Kumar, S., and Thompson, W.F. (2006). A modified protocol for rapid DNA isolation from plant tissues using cetyltrimethylammonium bromide. Nat. Protoc. **1**: 2320–2325.

Allorent, G., Osorio, S., Vu, J.L., Falconet, D., Jouhet, J., Kuntz, M., Fernie, A.R., Lerbs-Mache, S., Macherel, D., Courtois, F., and Finazzi, G. (2015). Adjustments of embryonic photosynthetic activity modulate seed fitness in Arabidopsis thaliana. New Phytol. **205**: 707–19.

Arnon, D.I. and Chain, R.K. (1975). Regulation of ferredoxin-catalyzed photosynthetic phosphorylations. Proc. Natl. Acad. Sci. U. S. A. **72**: 4961–5.

Asada, K. (2000). The water-water cycle as alternative photon and electron sinks. Philos. Trans. R. Soc. B Biol. Sci. **355**: 1419–1431.

Avenson, T.J., Cruz, J.A., Kanazawa, A., and Kramer, D.M. (2005). Regulating the proton budget of higher plant photosynthesis. Proc. Natl. Acad. Sci. U. S. A. **102**: 9709–13.

Bellan, A., Bucci, F., Perin, G., Alboresi, A., and Morosinotto, T. (2019). Photosynthesis regulation in response to fluctuating light in the secondary endosymbiont alga Nannochloropsis gaditana. Plant Cell Physiol.

Chaux, F., Burlacot, A., Mekhalfi, M., Auroy, P., Blangy, S., Richaud, P., and Peltier, G. (2017). Flavodiiron Proteins Promote Fast and Transient O2Photoreduction inChlamydomonas. Plant Physiol. **174**: 1825–1836.

DalCorso, G., Pesaresi, P., Masiero, S., Aseeva, E., Schünemann, D., Finazzi, G., Joliot, P., Barbato, R., and Leister, D. (2008). A complex containing PGRL1 and PGR5 is involved in the switch between linear and cyclic electron flow in Arabidopsis. Cell **132**: 273–85.

Driever, S.M. and Baker, N.R. (2011). The water-water cycle in leaves is not a major alternative electron sink for dissipation of excess excitation energy when CO2 assimilation is restricted. Plant. Cell Environ. **34**: 837–846.

Edwards, K., Johnstone, C., and Thompson, C. (1991). A simple and rapid method for the preparation of plant genomic DNA for PCR analysis. Nucleic Acids Res. **19**: 1349.

Endo, T., Shikanai, T., Takabayashi, A., Asada, K., and Sato, F. (1999). The role of chloroplastic NAD(P)H dehydrogenase in photoprotection. FEBS Lett. **457**: 5–8.

Gerotto, C., Alboresi, A., Giacometti, G.M.G.M., Bassi, R., and Morosinotto, T. (2012). Coexistence of plant and algal energy dissipation mechanisms in the moss Physcomitrella patens. New Phytol. **196**: 763–73.

Gerotto, C., Alboresi, A., Meneghesso, A., Jokel, M., Suorsa, M., Aro, E.-M.E.M., and Morosinotto, T. (2016). Flavodiiron proteins act as safety valve for electrons in Physcomitrella patens (National Academy of Sciences).

Hertle, A.P., Blunder, T., Wunder, T., Pesaresi, P., Pribil, M., Armbruster, U., and Leister, D. (2013). PGRL1 is the elusive ferredoxin-plastoquinone reductase in photosynthetic cyclic electron flow. Mol. Cell **49**: 511–23.

Ilík, P., Pavlovič, A., Kouřil, R., Alboresi, A., Morosinotto, T., Allahverdiyeva, Y., Aro, E.-M., Yamamoto, H., and Shikanai, T. (2017). Alternative electron transport mediated by flavodiiron proteins is operational in organisms from cyanobacteria up to gymnosperms. New Phytol. **214**.

Ishikawa, N., Endo, T., and Sato, F. (2008). Electron transport activities of Arabidopsis thaliana mutants with impaired chloroplastic NAD(P)H dehydrogenase. J. Plant Res. **121**: 521–526.

Ishikawa, N., Takabayashi, A., Noguchi, K., Tazoe, Y., Yamamoto, H., von Caemmerer, S., Sato, F., and Endo, T. (2016). NDH-Mediated Cyclic Electron Flow Around Photosystem I is Crucial for C $_4$ Photosynthesis. Plant Cell Physiol. **57**: 2020–2028.

Järvi, S., Suorsa, M., and Aro, E.-M. (2015). Photosystem II repair in plant chloroplasts — Regulation, assisting proteins and shared components with photosystem II biogenesis. Biochim. Biophys. Acta - Bioenerg. **1847**: 900–909.

Järvi, S., Suorsa, M., Paakkarinen, V., and Aro, E.-M. (2011). Optimized native gel systems for separation of thylakoid protein complexes: novel super- and mega-complexes. Biochem. J. **439**: 207–14.

Joliot, P., Béal, D., and Joliot, A. (2004). Cyclic electron flow under saturating excitation of dark-adapted Arabidopsis leaves. Biochim. Biophys. Acta **1656**: 166–76.

Joliot, P. and Johnson, G.N. (2011). Regulation of cyclic and linear electron flow in higher plants. Proc. Natl. Acad. Sci. U. S. A. **108**: 13317–22.

Kügler, M., Jänsch, L., Kruft, V., Schmitz, U.K., and Braun, H.P. (1997). Analysis of the chloroplast protein complexes by blue-native polyacrylamide gel electrophoresis (BN-PAGE). Photosynth. Res. **53**: 35–44.

Kukuczka, B., Magneschi, L., Petroutsos, D., Steinbeck, J., Bald, T., Powikrowska, M.,

Fufezan, C., Finazzi, G., and Hippler, M. (2014). Proton Gradient Regulation5-Like1-Mediated Cyclic Electron Flow Is Crucial for Acclimation to Anoxia and Complementary to Nonphotochemical Quenching in Stress Adaptation. Plant Physiol. **165**: 1604–1617.

Kulheim, C., Agren, J., Jansson, S., Külheim, C., Agren, J., and Jansson, S. (2002). Rapid regulation of light harvesting and plant fitness in the field. Science **297**: 91–3.

Larosa, V., Meneghesso, A., La Rocca, N., Steinbeck, J., Hippler, M., Szabò, I., and Morosinotto, T. (2018). Mitochondria Affect Photosynthetic Electron Transport and Photosensitivity in a Green Alga. Plant Physiol. **176**: 2305–2314.

Munekage, Y., Hashimoto, M., Miyake, C., Tomizawa, K., Endo, T., Tasaka, M., and Shikanai, T. (2004). Cyclic electron flow around photosystem I is essential for photosynthesis. Nature **429**: 579–82.

Munekage, Y., Hojo, M., Meurer, J., Endo, T., Tasaka, M., and Shikanai, T. (2002). PGR5 is involved in cyclic electron flow around photosystem I and is essential for photoprotection in Arabidopsis. Cell **110**: 361–71.

Nawrocki, W.J., Bailleul, B., Cardol, P., Rappaport, F., Wollman, F.-A., and Joliot, P. (2019). Maximal cyclic electron flow rate is independent of PGRL1 in Chlamydomonas. Biochim. Biophys. acta. Bioenerg.

Peltier, G., Aro, E.-M., and Shikanai, T. (2016). NDH-1 and NDH-2 Plastoquinone Reductases in Oxygenic Photosynthesis. Annu. Rev. Plant Biol. **67**: 55–80.

Peltier, G., Tolleter, D., Billon, E., and Cournac, L. (2010). Auxiliary electron transport pathways in chloroplasts of microalgae. Photosynth. Res. **106**: 19–31.

Shikanai, T. (2014). Central role of cyclic electron transport around photosystem I in the regulation of photosynthesis. Curr. Opin. Biotechnol. **26**: 25–30.

Shikanai, T. (2016). Regulatory network of proton motive force: contribution of cyclic electron transport around photosystem I. Photosynth. Res. **129**: 1–8.

Shikanai, T., Endo, T., Hashimoto, T., Yamada, Y., Asada, K., and Yokota, A. (1998). Directed disruption of the tobacco ndhB gene impairs cyclic electron flow around photosystem I. Proc. Natl. Acad. Sci. U. S. A. **95**: 9705–9.

Shikanai, T. and Yamamoto, H. (2017). Contribution of Cyclic and Pseudo-cyclic Electron Transport to the Formation of Proton Motive Force in Chloroplasts. Mol. Plant **10**: 20–29.

Shimakawa, G., Murakami, A., Niwa, K., Matsuda, Y., Wada, A., and Miyake, C. (2018). Comparative analysis of strategies to prepare electron sinks in aquatic photoautotrophs. Photosynth. Res.

Storti, M., Alboresi, A., Gerotto, C., Aro, E.-M., Finazzi, G., and Morosinotto, T. (2019). Role

of cyclic and pseudo-cyclic electron transport in response to dynamic light changes in Physcomitrella patens. Plant. Cell Environ. **42**: 1590–1602.

Suorsa, M., Järvi, S., Grieco, M., Nurmi, M., Pietrzykowska, M., Rantala, M., Kangasjärvi, S., Paakkarinen, V., Tikkanen, M., Jansson, S., and Aro, E.-M. (2012). PROTON GRADIENT REGULATION5 is essential for proper acclimation of Arabidopsis photosystem I to naturally and artificially fluctuating light conditions. Plant Cell **24**: 2934–48.

Terashima, I., Funayama, S., and Sonoike, K. (1994). The site of photoinhibition in leaves of Cucumis sativus L. at low temperatures is photosystem I, not photosystem II. Planta **193**.

Tikkanen, M., Mekala, N.R., and Aro, E.-M. (2014). Photosystem II photoinhibition-repair cycle protects Photosystem I from irreversible damage. Biochim. Biophys. Acta **1837**: 210–5.

Tiwari, A., Mamedov, F., Grieco, M., Suorsa, M., Jajoo, A., Styring, S., Tikkanen, M., and Aro, E.-M. (2016). Photodamage of iron–sulphur clusters in photosystem I induces non-photochemical energy dissipation. Nat. Plants: 16035.

Tjus, S.E., Møller, B.L., and Scheller, H. V (1998). Photosystem I is an early target of photoinhibition in barley illuminated at chilling temperatures. Plant Physiol. **116**: 755–64.

Wada, S., Yamamoto, H., Suzuki, Y., Yamori, W., Shikanai, T., and Makino, A. (2018). Flavodiiron Protein Substitutes for Cyclic Electron Flow without Competing CO2 Assimilation in Rice. Plant Physiol. **176**: 1509–1518.

Yamamoto, H., Takahashi, S., Badger, M.R., and Shikanai, T. (2016). Artificial remodelling of alternative electron flow by flavodiiron proteins in Arabidopsis. Nat. plants **2**: 16012.

Yamori, W. and Shikanai, T. (2016). Physiological Functions of Cyclic Electron Transport Around Photosystem I in Sustaining Photosynthesis and Plant Growth. Annu. Rev. Plant Biol. **67**: 81–106.

Yamori, W., Shikanai, T., and Makino, A. (2015). Photosystem I cyclic electron flow via chloroplast NADH dehydrogenase-like complex performs a physiological role for photosynthesis at low light. Sci. Rep. **5**: 13908.

Figure legends.

Figure 1. Impact of mutations on the photosynthetic apparatus composition. A) Immunoblot analysis of various proteins of the photosynthetic apparatus. A total extract amount equivalent to 2 µg of Chl (for FLVB, PsaD, D2, CP47, Cyt f, γATpase, PSBS, and LHCSR) and 4 µg of Chl (for PSAA, NDHM and FLVA) was loaded for each sample. In the case of WT, 2X and 0.5X indicate the loading of twice and half the amount of extract, respectively. B) Clear native PAGE (4-12%

493 acrylamide), thylakoids solubilized with mild detergent (0.75% αDM). For each lane, a volume of
494 extract corresponding to 15 µg of Chl was loaded. C) PSI/PSII ratio quantified from the ECS signal
495 obtained after the application of a single turnover pulse (see Materials and Methods). For each
496 genotype, the average result from two independent lines is reported with a total of n > 6
497 independent biological replicates (one-way ANOVA, p<0.001 is indicated by an asterisk).
498
499 **Figure 2. Photosynthetic electron transfer in P. patens plants**. A-B) Electron transport rate of
500 dark-acclimated plants grown under dim light, calculated from the electrochromic shift signal under
501 saturating light (940 µmol photons m^{-2} s^{-1}). Activity was normalized to the total photosystem
502 (PSI+PSII) content. Standard deviation is also reported (n > 7). All genotypes are significantly
503 different from WT after 0.8 seconds of illumination, while only flva-pgrl1-ndhm is different from
504 WT after 300 seconds (T-test, p < 0.01, indicated by an asterisk). C) Proton motive force (pmf)
505 estimated from the ECS signal at a steady state (after 5 minutes of illumination). Traces are shown
506 in Figure S4. flva-pgrl1-ndhm is significantly different from WT and all double mutants (n > 7). D)
507 Gross oxygen evolution under saturating (800 µmol photons m^{-2} s^{-1}) light. E) Oxygen consumption
508 in the dark measured in dark-acclimated plants. An asterisk indicates statistical significance (one-
509 way ANOVA, p<0.001, n>15). F) The PSII quantum yield, as indicated by F_v/F_m, was evaluated in
510 plants cultivated in control conditions (n >10, p < 0.001). In C-F plots, the 25th and 75th percentiles
511 are delimited by boxes, while whiskers indicate the minimum and maximum values. G-H) PSI
512 yield, PSI donor (Y ND) and acceptor side (Y NA) limitation upon exposure to limiting (G, 50
513 µmol photons m^{-2} s^{-1}) or saturating (H, 1000 µmol photons m^{-2} s^{-1}) light. The full kinetics are shown
514 in Figure S5. Data are shown as the average ± SD, and asterisks indicate values significantly
515 different from those in the WT (n > 4, p < 0.001). The WT is shown in black, flva-pgrl1 in cyan,
516 flva-ndhm in green, pgrl1-ndhm in blue and flva-pgrl1-ndhm in red.
517
518 **Figure 3. Impact of the depletion of electron transport regulation on *P. patens* growth.** *P.*
519 *patens* WT and mutant plants were grown under illumination of different intensities, ranging from
520 limiting (LL, 10 µmol photons m^{-2} s^{-1}) to optimal (CL, 50 µmol photons m^{-2} s^{-1}) or excessive (ML
521 and HL, 150 and 500 µmol photons m^{-2} s^{-1}). Cells were also exposed to light fluctuations (FL) in
522 which 3 minutes at 525 µmol photons m^{-2} s^{-1} was followed by 9 minutes at 25 µmol photons m^{-2} s^{-1}.
523 Representative images (A) and growth quantification (B) of 21-day-old plants. Images of plants
524 showing statistically significantly different growth from the WT are highlighted in green. Examples
525 of growth curves are shown in Supplementary Figure S7. In B, the plot depicts the median and 25-
526 75 percentiles in boxes and the minimum and maximum values as whiskers, with individual data

527 points superimposed on the boxes. WT is shown in black, *flva-pgrl1* in cyan, *flva-ndhm* in green,
528 *pgrl1-ndhm* in blue and *flva-pgrl1-ndhm* in red. Asterisks indicate genotypes with significant
529 differences from WT when grown in the same conditions (one-way ANOVA, n = 8-21, $p < 0.001$).
530
531 **Figure 4. Growth and active photosystem content in WT and *flva-pgrl1-ndhm* KO mutants**
532 **under different conditions.** A) WT and *flva-pgrl1-ndhm* plants were cultivated at 50 µmol photons
533 m^{-2} s^{-1} with different media: minimum medium ($PpNO_3$), rich medium ($PpNH_4$) and minimum
534 medium with the addition of ammonium tartrate (0.05%), glucose (0.5%), sucrose (0.5%) and
535 mannitol (0.5%). B) WT and *flva-pgrl1-ndhm* KO growth in an atmosphere enriched with 5% CO_2
536 with 24 hours of continuous illumination in control conditions using plants propagated for at least 3
537 weeks under low illumination (LL, 10 µmol m^{-2} s^{-1}). In both A-B, growth is normalized to the area
538 of WT plants grown in $PpNO_3$ medium under a 16 h light/ 8 h dark photoperiod at 50 µmol photons
539 m^{-2} s^{-1}. The plot depicts the median and 25-75 percentiles in boxes and the minimum and maximum
540 values as whiskers, with individual data points superimposed on the boxes. For each condition, WT
541 is shown in black, and *flva-pgrl1-ndhm* KO is shown in red. C) Spectroscopic quantification of the
542 active PSI / PSII ratio in WT and *flva-pgrl1-ndhm* KO plants cultivated in the presence of glucose
543 and in plants propagated under very low illumination. For all samples, between 4 and 8 independent
544 biological replicates were performed.

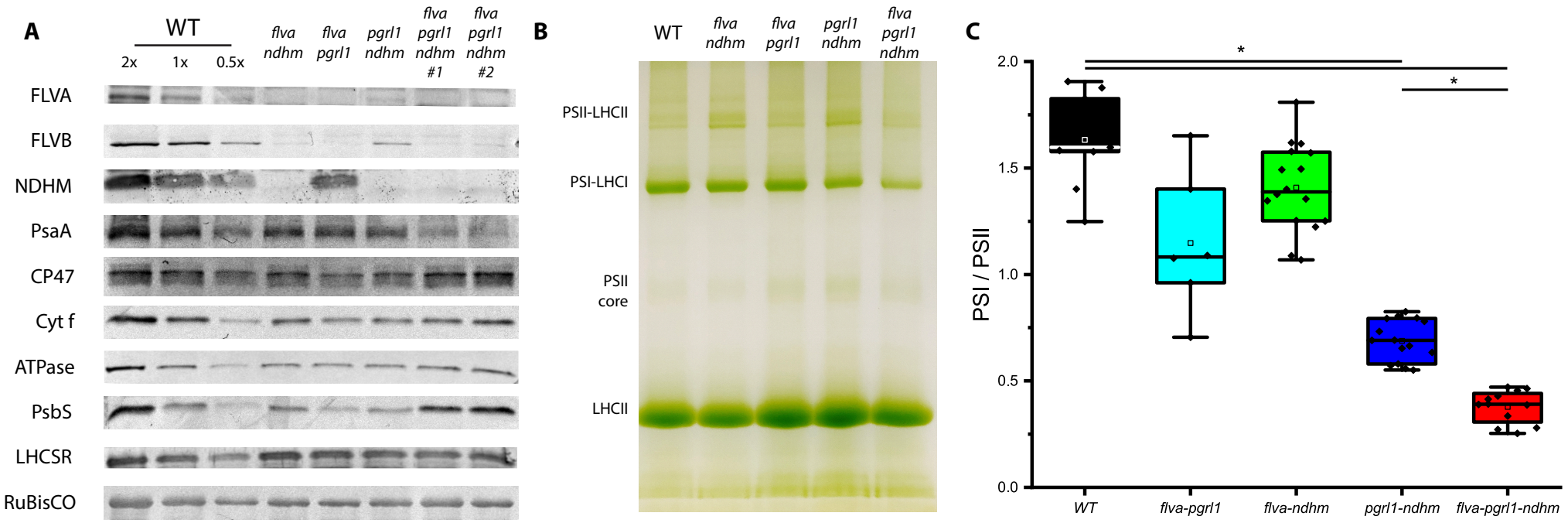

Figure 1. Impact of mutations on the photosynthetic apparatus composition. A) Immunoblot analysis of various proteins of the photosynthetic apparatus. A total extract amount equivalent to 2 µg of Chl (for FLVB, PsaD, D2, CP47, Cyt f, γATpase, PSBS, and LHCSR) and 4 µg of Chl (for PSAA, NDHM and FLVA) was loaded for each sample. In the case of WT, 2X and 0.5X indicate the loading of twice and half the amount of extract, respectively. B) Clear native PAGE (4-12% acrylamide), thylakoids solubilized with mild detergent (0.75% αDM). For each lane, a volume of extract corresponding to 15 µg of Chl was loaded. C) PSI/PSII ratio quantified from the ECS signal obtained after the application of a single turnover pulse (see Materials and Methods). For each genotype, the average result from two independent lines is reported with a total of n > 6 independent biological replicates (one-way ANOVA, $p<0.001$ is indicated by an asterisk).

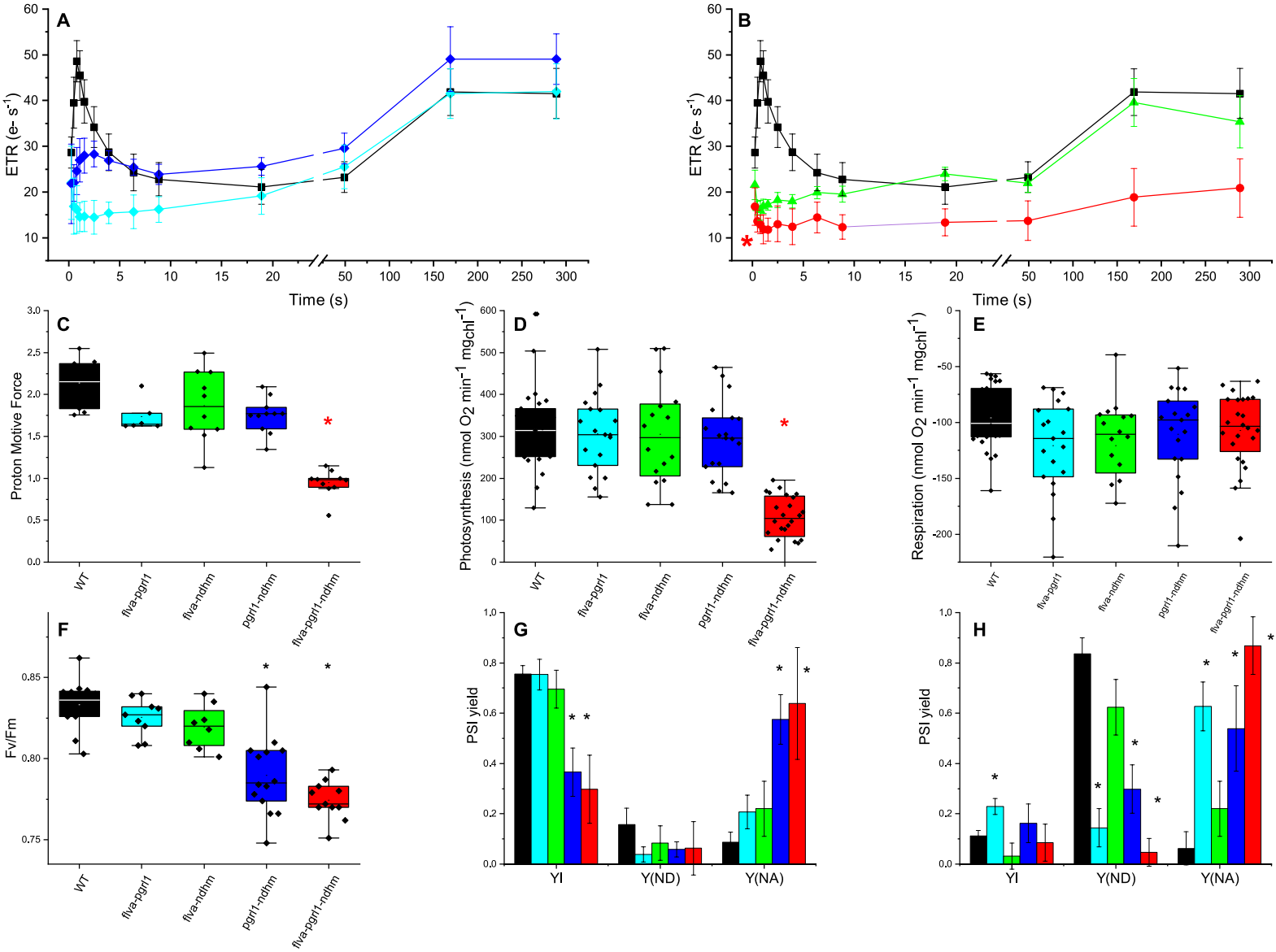

Figure 2. Photosynthetic electron transfer in P. patens plants. A-B) Electron transport rate of dark-acclimated plants grown under dim light, calculated from the electrochromic shift signal under saturating light (940 µmol photons m-2 s-1). Activity was normalized to the total photosystem (PSI+PSII) content. Standard deviation is also reported (n > 7). All genotypes are significantly different from WT after 0.8 seconds of illumination, while only flva-pgrl1-ndhm is different from WT after 300 seconds (T-test, $p < 0.01$, indicated by an asterisk). C) Proton motive force (pmf) estimated from the ECS signal at a steady state (after 5 minutes of illumination). Traces are shown in Figure S4. flva-pgrl1-ndhm is significantly different from WT and all double mutants (n > 7). D) Gross oxygen evolution under saturating (800 µmol photons m-2 s-1) light. E) Oxygen consumption in the dark measured in dark-acclimated plants. An asterisk indicates statistical significance (one-way ANOVA, $p<0.001$, $n>15$). F) The PSII quantum yield, as indicated by Fv/Fm, was evaluated in plants cultivated in control conditions (n >10, $p < 0.001$). In C-F plots, the 25th and 75th percentiles are delimited by boxes, while whiskers indicate the minimum and maximum values. G-H) PSI yield, PSI donor (Y ND) and acceptor side (Y NA) limitation upon exposure to limiting (G, 50 µmol photons m-2 s-1) or saturating (H, 1000 µmol photons m-2 s-1) light. The full kinetics are shown in Figure S5. Data are shown as the average ± SD, and asterisks indicate values significantly different from those in the WT (n > 4, $p < 0.001$). The WT is shown in black, flva-pgrl1 in cyan, flva-ndhm in green, pgrl1-ndhm in blue and flva-pgrl1-ndhm in red.

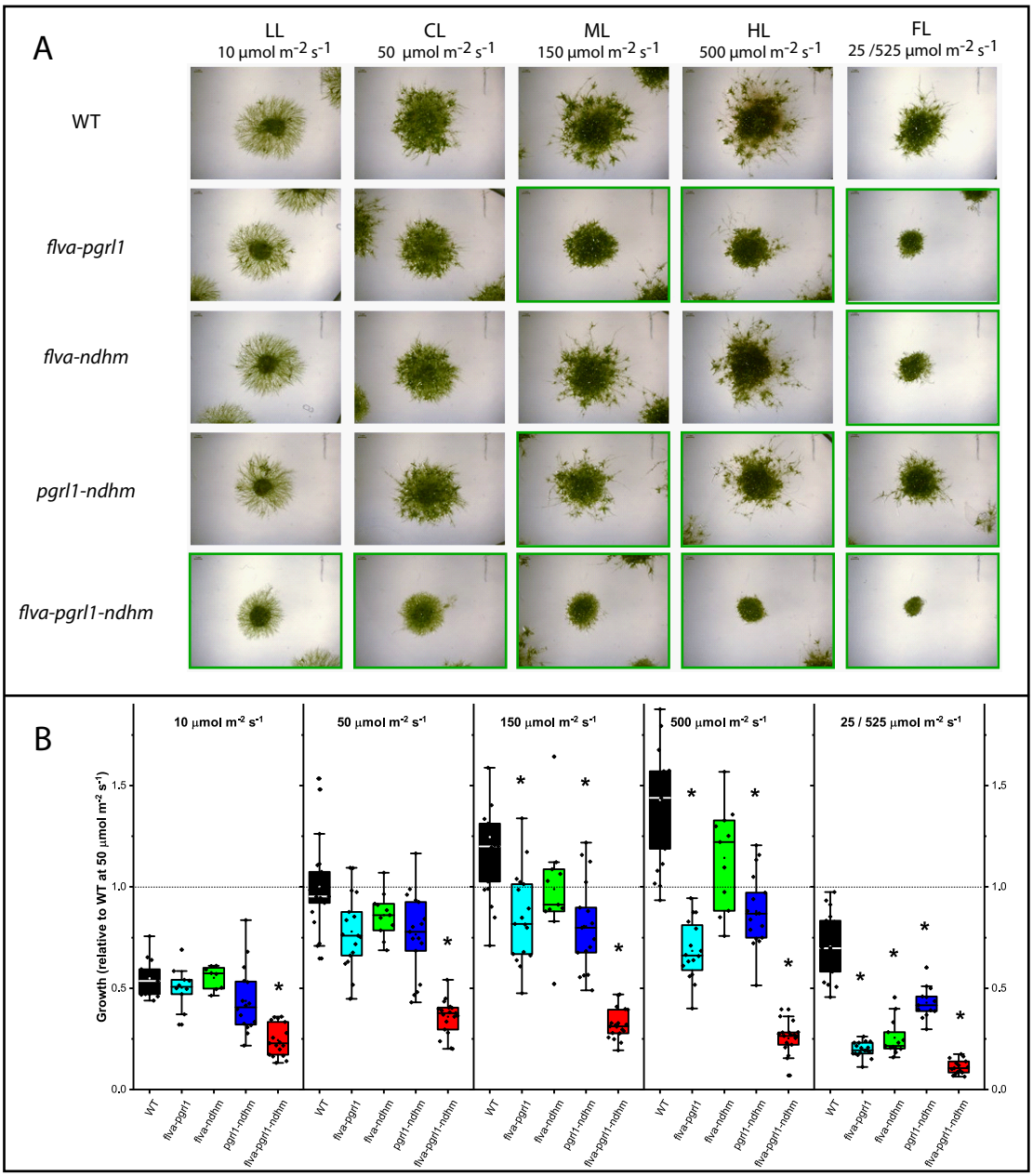

Figure 3. Impact of the depletion of electron transport regulation on P. patens growth. P. patens WT and mutant plants were grown under illumination of different intensities, ranging from limiting (LL, 10 µmol photons m-2 s-1) to optimal (CL, 50 µmol photons m-2 s-1) or excessive (ML and HL, 150 and 500 µmol photons m-2 s-1). Cells were also exposed to light fluctuations (FL) in which 3 minutes at 525 µmol photons m-2 s-1 was followed by 9 minutes at 25 µmol photons m-2 s-1. Representative images (A) and growth quantification (B) of 21-day-old plants. Images of plants showing statistically significantly different growth from the WT are highlighted in green. Examples of growth curves are shown in Supplementary Figure S7. In B, the plot depicts the median and 25-75 percentiles in boxes and the minimum and maximum values as whiskers, with individual data points superimposed on the boxes. WT is shown in black, flva-pgrl1 in cyan, flva-ndhm in green, pgrl1-ndhm in blue and flva-pgrl1-ndhm in red. Asterisks indicate genotypes with significant differences from WT when grown in the same conditions (one-way ANOVA, n = 8-21, $p < 0.001$).

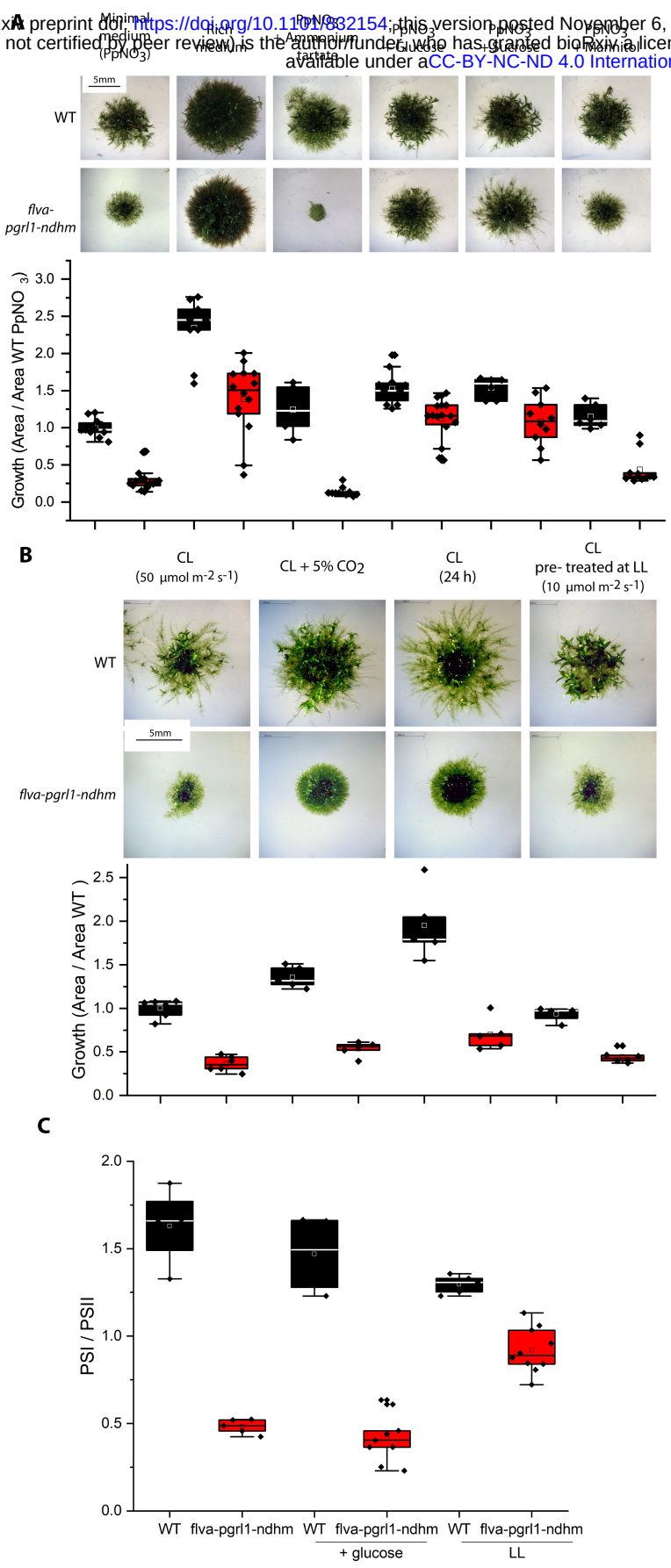

Figure 4. Growth and active photosystem content in WT and flva-pgrl1-ndhm KO mutants under different conditions. A) WT and flva-pgrl1-ndhm plants were cultivated at 50 µmol photons m-2 s-1 with different media: minimum medium (PpNO3), rich medium (PpNH4) and minimum medium with the addition of ammonium tartrate (0.05%), glucose (0.5%), sucrose (0.5%) and mannitol (0.5%). B) WT and flva-pgrl1-ndhm KO growth in an atmosphere enriched with 5% CO2 with 24 hours of continuous illumination in control conditions using plants propagated for at least 3 weeks under low illumination (LL, 10 µmol m-2 s-1). In both A-B, growth is normalized to the area of WT plants grown in PpNO3 medium under a 16 h light/ 8 h dark photoperiod at 50 µmol photons m-2 s-1. The plot depicts the median and 25-75 percentiles in boxes and the minimum and maximum values as whiskers, with individual data points superimposed on the boxes. For each condition, WT is shown in black, and flva-pgrl1-ndhm KO is shown in red. C) Spectroscopic quantification of the active PSI / PSII ratio in WT and flva-pgrl1-ndhm KO plants cultivated in the presence of glucose and in plants propagated under very low illumination. For all samples, between 4 and 8 independent biological replicates were performed.

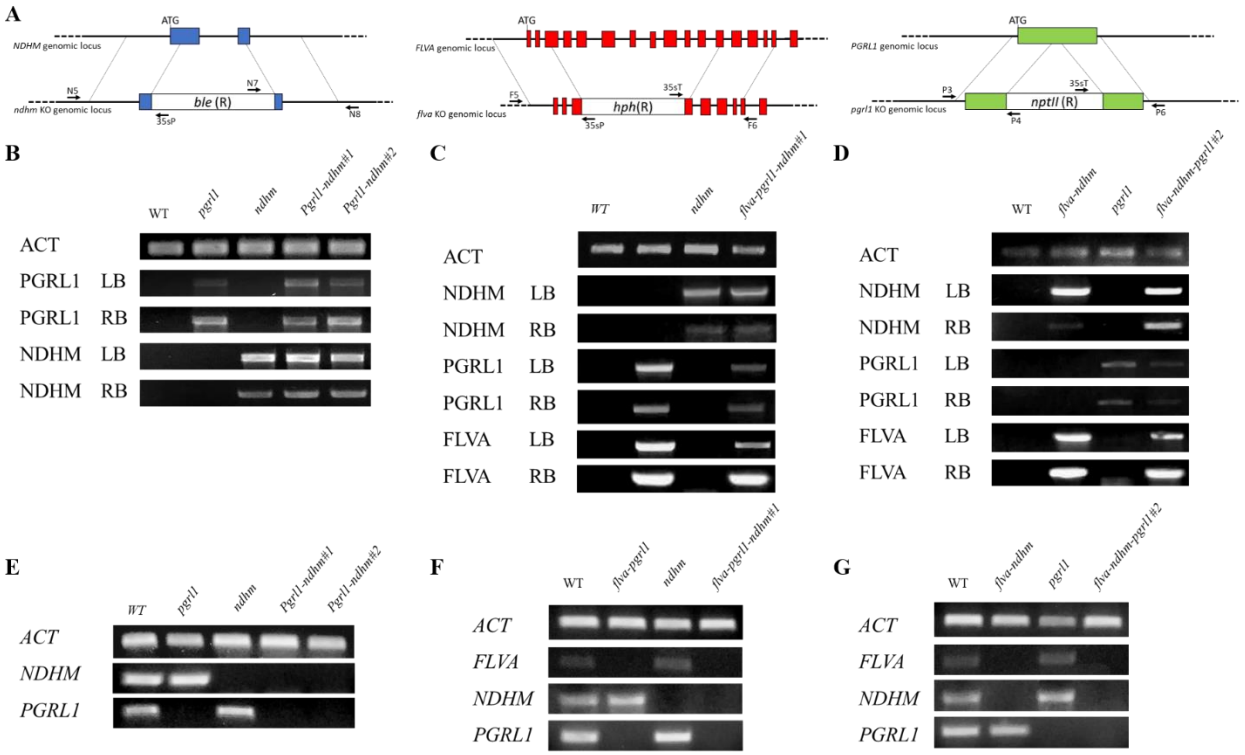

Figure S1. Isolation of double and triple KO *P. patens* plants. A) Scheme of the KO generation by homologous recombination. Two homologous regions drive the insertion of the resistance cassette disrupting the target gene. NDHM, PGRL1 and FLV exons are respectively shown in blue, red and green. Ble, hph and nptII genes confer respectively the resistance to zeocin, hygromicine-B and G418. B- D) Homologous recombination event was first verified by PCR on gDNA confirming insertion of resistance cassettes in the target *loci*. Left and right borders (LB / RB) PCR were performed with one primer annealing outside the insertion locus and one annealing on the resistance cassette as shown in A. Primer sequences are reported in Table S1. E-G) Expression of the target genes was assessed by RT-PCR. Single KO as well as *flva-pgrl1* and *flva-ndhm* KO isolation was previously described (Storti et al., 2019), here results for *pgrl1-ndhm* and *flva-pgrl1-ndhm* KO are reported. Two independent lines for each genotype are shown. In the case of *flva-pgrl1-ndhm* KO the two independent lines were generated starting from two distinct mutant backgrounds (*flva-pgrl1* and *flva-ndhm* respectively in C, D).

Gene	Primer name	Sequence	Use
FLVA	F5	CGCTGAAATCACCAGTCTCTCT	KO screening
FLVA	F6	GCTAAGCGCAGCAACACTTT	KO screening
PGRL1	P3	TAAAAAATCAAGTGATGTTATCCA	KO screening
PGRL1	P6	AGGAACTGAGAGTACATATGGTGA	KO screening
NDHM	N5	TTGGAAGTCTGTTCACGCTTT	KO screening
NDHM	N8	TTCTGCCAATAGGATGTGAGG	KO screening
35s promoter	35sP	GTGTCGTGCTCCACCATGT	KO screening
35s terminator	35sT	CGCTGAAATCACCAGTCTCTCT	KO screening
nptII	P4	GGCAATGGAATCCGAGGAGGT	KO screening
ble	N7	CCCCGCTTAAAATTGGTAT	KO screening
FLVA	FF	TTTGGCTCTTTCGGGTGGAG	RT-PCR
FLVA	FR	GACGGTTTTCGCCAGGTTTG	RT-PCR
PGRL1	PF	CCATCCAACAACGTCAAA	RT-PCR
PGRL1	PR	TTCAGCCAAAGGGCTCTCTA	RT-PCR
NDHM	NF	AGTGTCCTCCGCTTTTCTCA	RT-PCR
NDHM	NR	CTCCGTCAAATCTGCACCTG	RT-PCR
ACTIN2	ACTIN2F	GCGAAGAGCGAGTATGACGAG	RT-PCR
ACTIN2	ACTIN2R	AGCCACGAATCTAACTTGTGATG	RT-PCR

Table S1. Primers employed in this work.

Table S2. Pigment composition of *P. patens* WT and mutant plants. Chlorophyll (Chl) a/b ratio, Chl / carotenoids (car) ratio and total Chl content is shown. Standard deviation is also reported and asterisk indicates statistically significant differences ($n > 5$, $p < 0.01$).

	Chl a/Chl b	**chl/car**	**Chl content ($\mu g\ mg^{-1}$ dry weight)**
WT	2.53 ± 0.10	3.74 ± 0.35	18.9 ± 4.6
flva-ndhm	2.50 ± 0.08	3.80 ± 0.22	21.6 ± 3.4
flva-pgrl1	2.49 ± 0.12	3.70 ± 0.36	19.6 ± 3.8
pgrl1-ndhm	2.51 ± 0.10	3.54 ± 0.35	17.8 ± 2.9
flva-pgrl1-ndhm	2.40 ± 0.11*	3.78 ± 0.67	21.5 ± 5.1

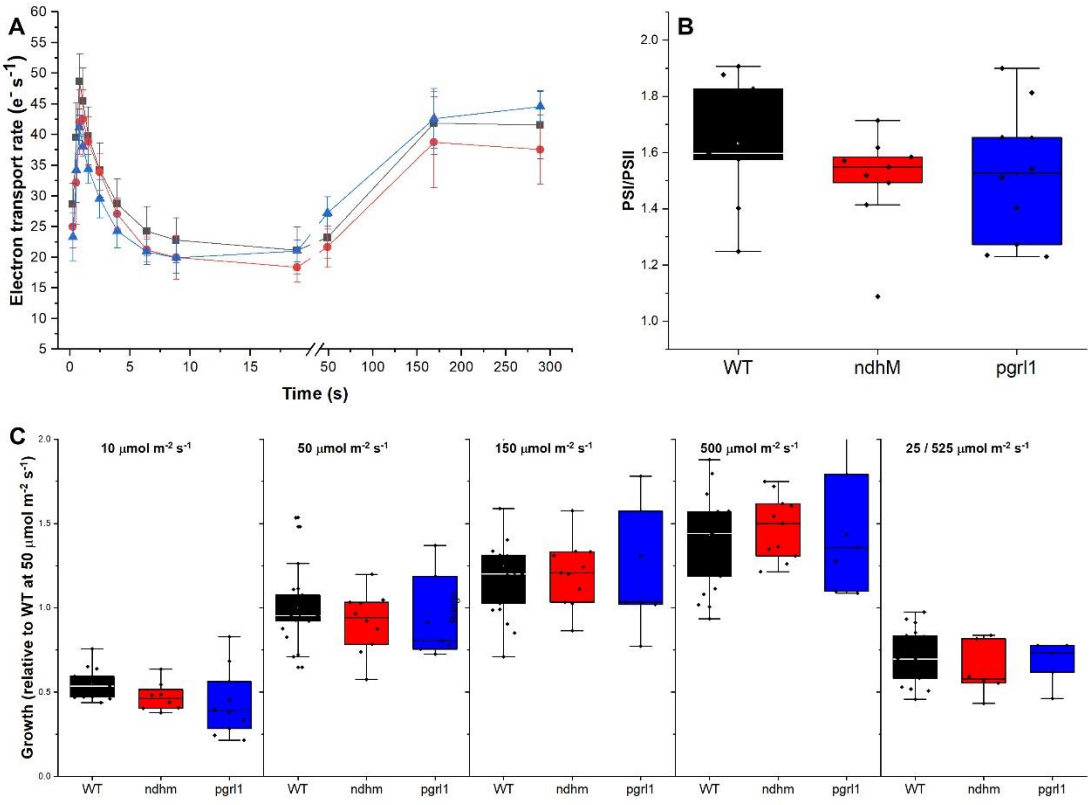

Figure S2. Phenotype of pgrl1 and ndhm KO. A) Electron transport rate, calculated from electrochromic shift, of dark acclimated plants after illumination with saturating light (940 µmol photons m^{-2} s^{-1}) for 300s. Electron transport was normalized to total charge separation capacity (thus to the activity of both PSI and PSII) quantified from single turnover pulse excitation. Data are represented as mean and standard deviation is also reported (n > 10). B) PSI/PSII ratio calculated from single pulse excitation. PSI contribution was measured in presence of DCMU that inhibits PSII activity. C) Quantification of the growth of *P. patens* WT and *pgrl1* and *ndhm* KO grown under illumination of different intensity: limiting (LL, 10 µmol photons m^{-2} s^{-1}), optimal (CL, 50 µmol photons m^{-2} s^{-1}), excess light (ML and HL, 150 and 500 µmol photons m^{-2} s^{-1}); or light fluctuations (FL, 3 minutes at 525 µmol photons m^{-2} s^{-1} and 9 minutes at 25 µmol photons m^{-2} s^{-1}). In B and C, plots depict median and 25-75 percentiles as boxes, minimum and maximum values as whiskers and outliers as external points, individual data points are also superimposed to the boxes. In all panels WT is shown in in black, *ndhm* in red and *pgrl1* in blue.

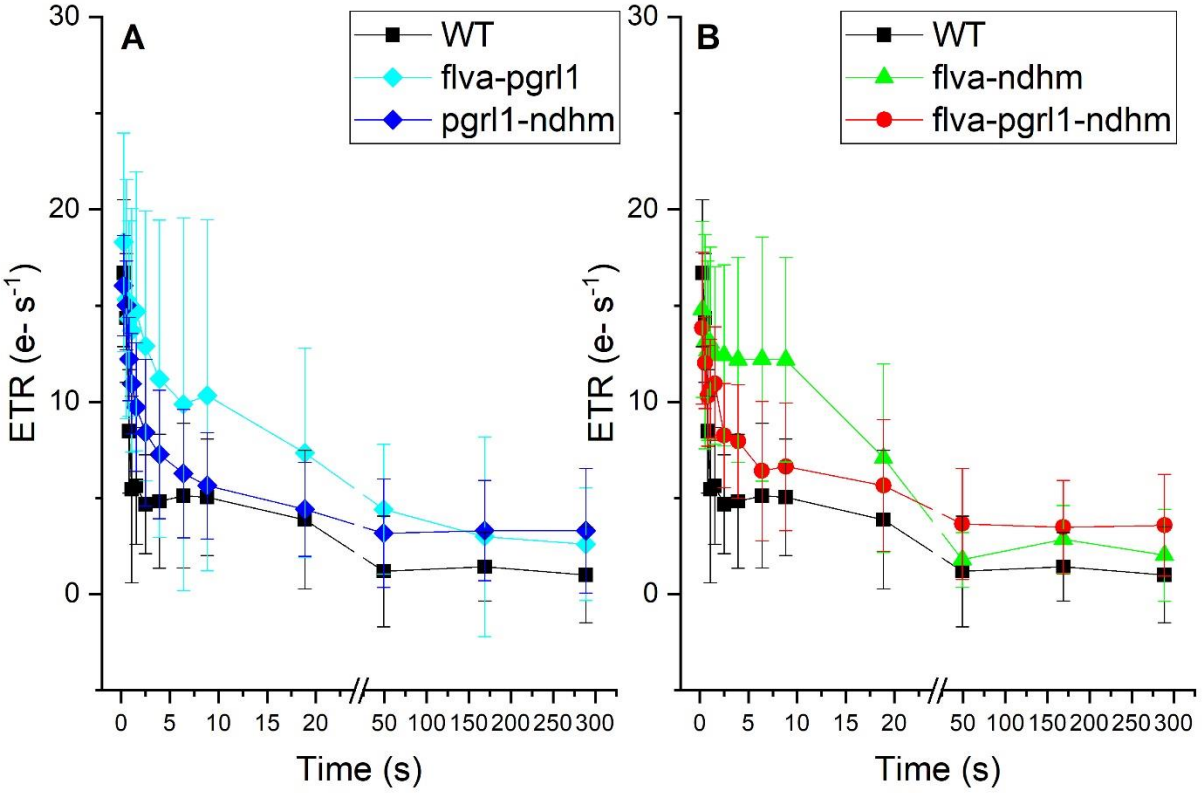

Figure S3. PSII independent electron transport. Photosynthetic electron transport, calculated from electrochromic shift signal, measured in the presence of the PSII inhibitor DCMU. Activity was normalized to total photosystems content (PSI+PSII). Mean values and standard deviation are reported (n > 6). WT is shown in in black, *flva-pgrl1* in cyan, *flva-ndhm* in green, *pgrl1-ndhm* in blue and *flva-pgrl1-ndhm* in red.

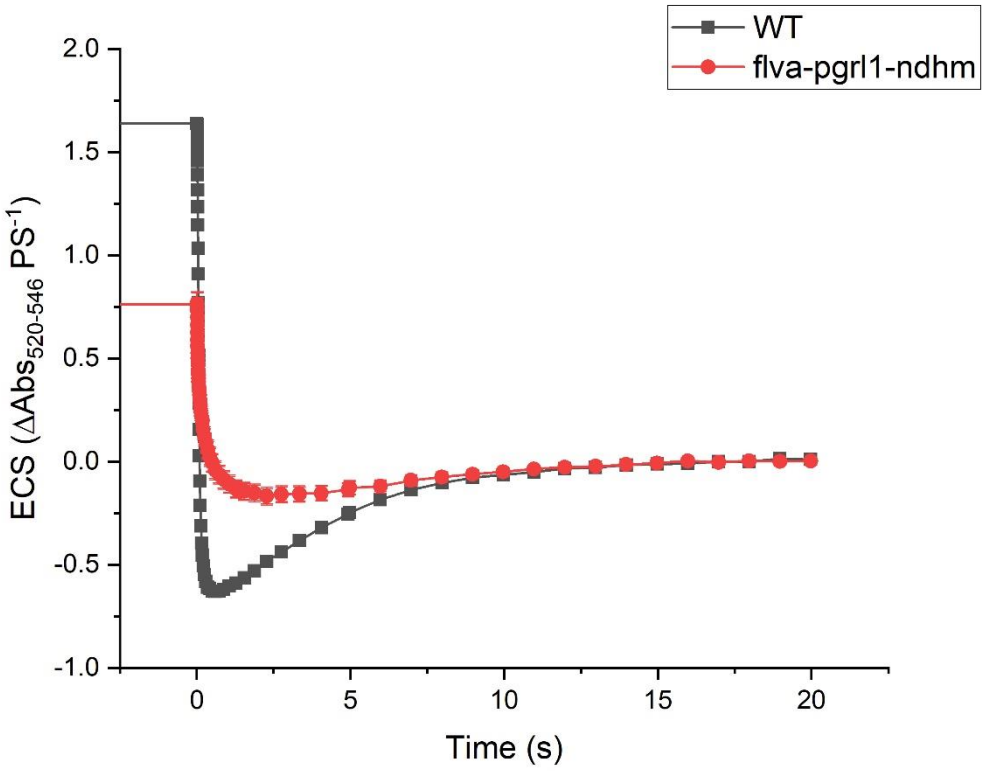

Figure S4. Examples of ECS traces in WT and *flva-pgrl1-ndhm* mutant. Dark adapted plants were subjected to 940 µmol photons m^{-2} s^{-1} for 300s before light was switch off (0 s). Relaxation of electrochromic shift signal (520-546 nm) in the dark is reported for WT (black) and *flva-pgrl1-ndhm* KO (red). ECS signal is normalized to total photosystem content (PSI+PSII) calculated from single flash turnover.

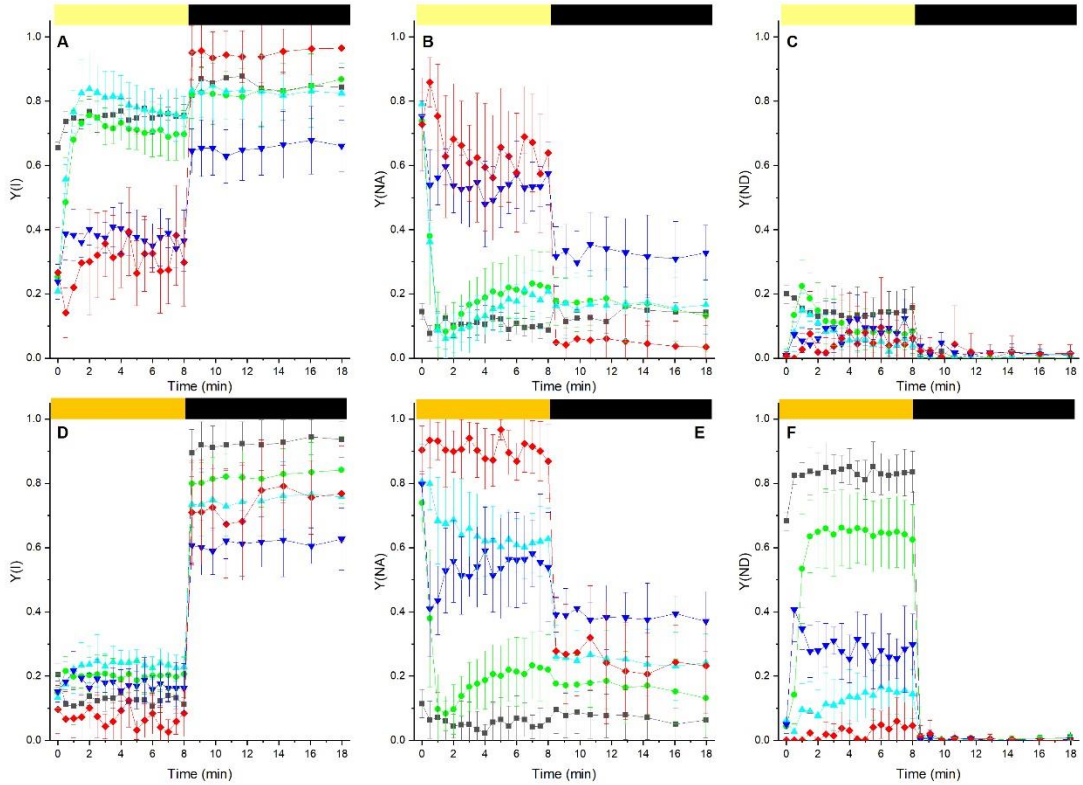

Figure S5. Photosystems I functionality under dim / High illumination. Yield of PSI (Y(I); A,D), PSI acceptor (Y(NA); B-E) and donor side limitation (Y(ND); C-F) were measured with Dual-PAM 100 under dim (50 µmol photons $m^{-2}s^{-1}$, A-C) or high (550 µmol photons $m^{-2}s^{-1}$, D-F) illumination. Actinic light (upper yellow bar) was switched off after 8 min. In all panels WT is shown in in black, *flva-pgrl1* in cyan, *flva-ndhm* in green, *pgrl1-ndhm* in blue and *flva-pgrl1-ndhm* in red. Data are shown as average ± SD (n > 4).

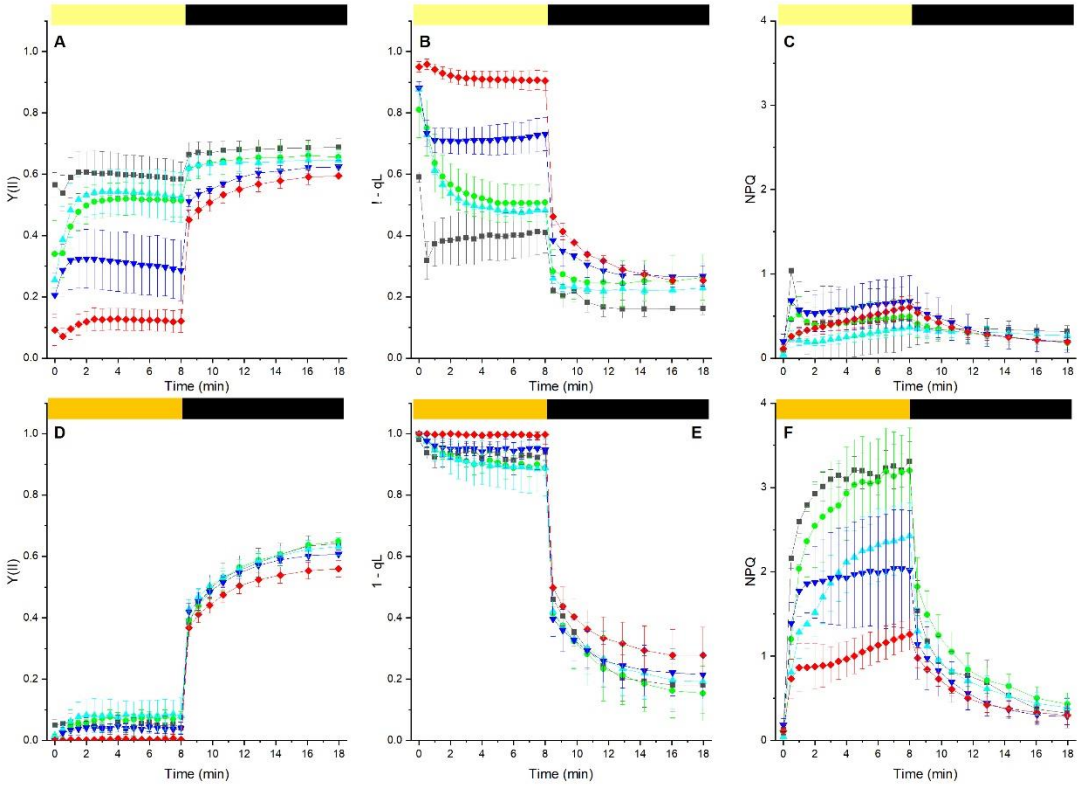

Figure S6. Photosystem II functionality under dim / High illumination. Yield of PSII (Y(II); A,D), PQ reox state (1-qL); B-E) and non-photochemical quenching (NPQ); C-F) were measured with Dual-PAM 100 under dim (50 µmol photons $m^{-2}s^{-1}$, A-C) or high (550 µmol photons $m^{-2}s^{-1}$, D-F) illumination. Actinic light (upper yellow bar) was switched off after 8 min. In all panels WT is shown in in black, *flva-pgrl1* in cyan, *flva-ndhm* in green, *pgrl1-ndhm* in blue and *flva-pgrl1-ndhm* in red. Data are shown as average ± SD (n > 4).

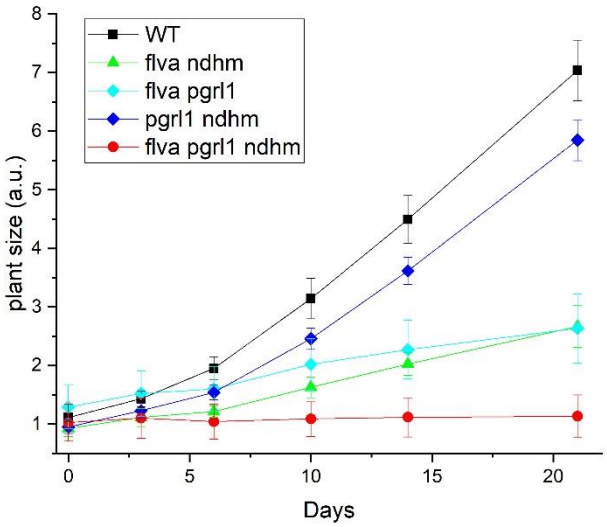

Figure S7. Example of growth curve *P. patens* mutants. *P. patens* WT and mutants were grown under light fluctuations (FL) where 3 minute at 525 µmol photons m^{-2} s^{-1} was followed by 9 minutes at 25 µmol photons m^{-2} s^{-1}. After 21 days (see Figure 1), plants were still actively growing. Plant growth was quantified from image analysis as detailed in (Storti et al., 2019), plant sizes were normalized to WT initial size at day 0. WT, *pgrl1-ndhm*, *pgrl1-flva*, *ndhm-flva* and triple *flva-pgrl1-ndhm* KO are shown respectively in black, blue, cyan, green and red.

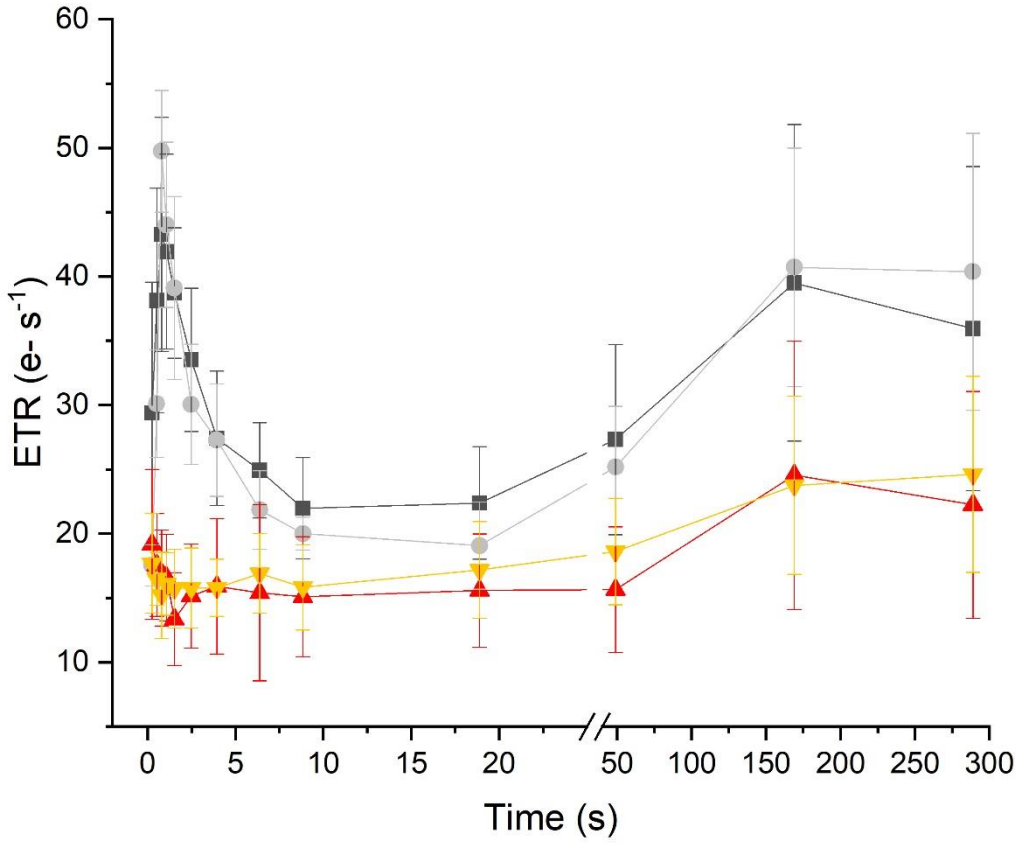

Figure S8. Photosynthetic ETR in plants grown heterotrophically. Electron transport rate, calculated from electrochromic shift signal, was measured on plants grown in $PpNO_3$ medium or $PpNO_3$ with the addiction of 0.5 % glucose. WT and *flva-pgrl1-ndhm* KO grown in $PpNO_3$ are represented respectively in black and red, WT and mutant grown in enriched medium are represented in grey and orange. Data are shown as average ± SD (n > 3).

Parsed Citations

Alboresi, A., Gerotto, C., Giacometti, G.M., Bassi, R., Morosinotto, T. (2010). Physcomitrella patens mutants affected on heat dissipation clarify the evolution of photoprotection mechanisms upon land colonization. Proc. Natl. Acad. Sci. U. S. A. 107: 11128–33.

Pubmed: Author and Title
Google Scholar: Author Only Title Only Author and Title

Alboresi, A., Storti, M., and Morosinotto, T. (2019). Balancing protection and efficiency in the regulation of photosynthetic electron transport across plant evolution. New Phytol. 221: 105–109.

Pubmed: Author and Title
Google Scholar: Author Only Title Only Author and Title

Allahverdiyeva, Y., Mustila, H., Ermakova, M., Bersanini, L., Richaud, P., Ajlani, G., Battchikova, N., Cournac, L., and Aro, E.-M. (2013). Flavodiiron proteins Flv1 and Flv3 enable cyanobacterial growth and photosynthesis under fluctuating light. Proc. Natl. Acad. Sci. U. S. A. 110: 4111–6.

Pubmed: Author and Title
Google Scholar: Author Only Title Only Author and Title

Allahverdiyeva, Y., Suorsa, M., Tikkanen, M., and Aro, E.-M.E.-M. (2015). Photoprotection of photosystems in fluctuating light intensities. J. Exp. Bot. 66: 2427–36.

Pubmed: Author and Title
Google Scholar: Author Only Title Only Author and Title

Allen, G.C., Flores-Vergara, M.A., Krasynanski, S., Kumar, S., and Thompson, W.F. (2006). A modified protocol for rapid DNA isolation from plant tissues using cetyltrimethylammonium bromide. Nat. Protoc. 1: 2320–2325.

Pubmed: Author and Title
Google Scholar: Author Only Title Only Author and Title

Allorent, G., Osorio, S., Vu, J.L., Falconet, D., Jouhet, J., Kuntz, M., Fernie, A.R., Lerbs-Mache, S., Macherel, D., Courtois, F., and Finazzi, G. (2015). Adjustments of embryonic photosynthetic activity modulate seed fitness in Arabidopsis thaliana. New Phytol. 205: 707–19.

Pubmed: Author and Title
Google Scholar: Author Only Title Only Author and Title

Arnon, D.I. and Chain, R.K. (1975). Regulation of ferredoxin-catalyzed photosynthetic phosphorylations. Proc. Natl. Acad. Sci. U. S. A. 72: 4961–5.

Pubmed: Author and Title
Google Scholar: Author Only Title Only Author and Title

Asada, K. (2000). The water-water cycle as alternative photon and electron sinks. Philos. Trans. R. Soc. B Biol. Sci. 355: 1419–1431.

Pubmed: Author and Title
Google Scholar: Author Only Title Only Author and Title

Avenson, T.J., Cruz, J.A., Kanazawa, A., and Kramer, D.M. (2005). Regulating the proton budget of higher plant photosynthesis. Proc. Natl. Acad. Sci. U. S. A. 102: 9709–13.

Pubmed: Author and Title
Google Scholar: Author Only Title Only Author and Title

Bellan, A., Bucci, F., Perin, G., Alboresi, A., and Morosinotto, T. (2019). Photosynthesis regulation in response to fluctuating light in the secondary endosymbiont alga Nannochloropsis gaditana. Plant Cell Physiol.

Pubmed: Author and Title
Google Scholar: Author Only Title Only Author and Title

Chaux, F., Burlacot, A., Mekhalfi, M., Auroy, P., Blangy, S., Richaud, P., and Peltier, G. (2017). Flavodiiron Proteins Promote Fast and Transient O2Photoreduction inChlamydomonas. Plant Physiol. 174: 1825–1836.

Pubmed: Author and Title
Google Scholar: Author Only Title Only Author and Title

DalCorso, G., Pesaresi, P., Masiero, S., Aseeva, E., Schünemann, D., Finazzi, G., Joliot, P., Barbato, R., and Leister, D. (2008). A complex containing PGRL1 and PGR5 is involved in the switch between linear and cyclic electron flow in Arabidopsis. Cell 132: 273–85.

Pubmed: Author and Title
Google Scholar: Author Only Title Only Author and Title

Driever, S.M. and Baker, N.R. (2011). The water-water cycle in leaves is not a major alternative electron sink for dissipation of excess excitation energy when CO2 assimilation is restricted. Plant. Cell Environ. 34: 837–846.

Pubmed: Author and Title
Google Scholar: Author Only Title Only Author and Title

Edwards, K., Johnstone, C., and Thompson, C. (1991). A simple and rapid method for the preparation of plant genomic DNA for PCR analysis. Nucleic Acids Res. 19: 1349.
Pubmed: Author and Title
Google Scholar: Author Only Title Only Author and Title

Endo, T., Shikanai, T., Takabayashi, A., Asada, K., and Sato, F. (1999). The role of chloroplastic NAD(P)H dehydrogenase in photoprotection. FEBS Lett. 457: 5–8.
Pubmed: Author and Title
Google Scholar: Author Only Title Only Author and Title

Gerotto, C., Alboresi, A., Giacometti, G.M.G.M., Bassi, R., and Morosinotto, T. (2012). Coexistence of plant and algal energy dissipation mechanisms in the moss Physcomitrella patens. New Phytol. 196: 763–73.
Pubmed: Author and Title
Google Scholar: Author Only Title Only Author and Title

Gerotto, C., Alboresi, A., Meneghesso, A., Jokel, M., Suorsa, M., Aro, E.-M.E.M., and Morosinotto, T. (2016). Flavodiiron proteins act as safety valve for electrons in Physcomitrella patens (National Academy of Sciences).

Hertle, A.P., Blunder, T., Wunder, T., Pesaresi, P., Pribil, M., Armbruster, U., and Leister, D. (2013). PGRL1 is the elusive ferredoxin-plastoquinone reductase in photosynthetic cyclic electron flow. Mol. Cell 49: 511–23.
Pubmed: Author and Title
Google Scholar: Author Only Title Only Author and Title

Ilík, P., Pavlovič, A., Kouřil, R., Alboresi, A., Morosinotto, T., Allahverdiyeva, Y., Aro, E.-M., Yamamoto, H., and Shikanai, T. (2017). Alternative electron transport mediated by flavodiiron proteins is operational in organisms from cyanobacteria up to gymnosperms. New Phytol. 214.
Pubmed: Author and Title
Google Scholar: Author Only Title Only Author and Title

Ishikawa, N., Endo, T., and Sato, F. (2008). Electron transport activities of Arabidopsis thaliana mutants with impaired chloroplastic NAD(P)H dehydrogenase. J. Plant Res. 121: 521–526.
Pubmed: Author and Title
Google Scholar: Author Only Title Only Author and Title

Ishikawa, N., Takabayashi, A., Noguchi, K., Tazoe, Y., Yamamoto, H., von Caemmerer, S., Sato, F., and Endo, T. (2016). NDH-Mediated Cyclic Electron Flow Around Photosystem I is Crucial for C 4 Photosynthesis. Plant Cell Physiol. 57: 2020–2028.
Pubmed: Author and Title
Google Scholar: Author Only Title Only Author and Title

Järvi, S., Suorsa, M., and Aro, E.-M. (2015). Photosystem II repair in plant chloroplasts - Regulation, assisting proteins and shared components with photosystem II biogenesis. Biochim. Biophys. Acta - Bioenerg. 1847: 900–909.
Pubmed: Author and Title
Google Scholar: Author Only Title Only Author and Title

Järvi, S., Suorsa, M., Paakkarinen, V., and Aro, E.-M. (2011). Optimized native gel systems for separation of thylakoid protein complexes: novel super- and mega-complexes. Biochem. J. 439: 207–14.
Pubmed: Author and Title
Google Scholar: Author Only Title Only Author and Title

Joliot, P., Béal, D., and Joliot, A. (2004). Cyclic electron flow under saturating excitation of dark-adapted Arabidopsis leaves. Biochim. Biophys. Acta 1656: 166–76.
Pubmed: Author and Title
Google Scholar: Author Only Title Only Author and Title

Joliot, P. and Johnson, G.N. (2011). Regulation of cyclic and linear electron flow in higher plants. Proc. Natl. Acad. Sci. U. S. A. 108: 13317–22.
Pubmed: Author and Title
Google Scholar: Author Only Title Only Author and Title

Kügler, M., Jänsch, L., Kruft, V., Schmitz, U.K., and Braun, H.P. (1997). Analysis of the chloroplast protein complexes by blue-native polyacrylamide gel electrophoresis (BN-PAGE). Photosynth. Res. 53: 35–44.
Pubmed: Author and Title
Google Scholar: Author Only Title Only Author and Title

Kukuczka, B., Magneschi, L., Petroutsos, D., Steinbeck, J., Bald, T., Powikrowska, M., Fufezan, C., Finazzi, G., and Hippler, M. (2014). Proton Gradient Regulation5-Like1-Mediated Cyclic Electron Flow Is Crucial for Acclimation to Anoxia and Complementary to Nonphotochemical Quenching in Stress Adaptation. Plant Physiol. 165: 1604–1617.
Pubmed: Author and Title
Google Scholar: Author Only Title Only Author and Title

Kulheim, C., Agren, J., Jansson, S., Külheim, C., Agren, J., and Jansson, S. (2002). Rapid regulation of light harvesting and plant

fitness in the field. Science 297: 91–3.
Pubmed: Author and Title
Google Scholar: Author Only Title Only Author and Title

Larosa, V., Meneghesso, A., La Rocca, N., Steinbeck, J., Hippler, M., Szabò, I., and Morosinotto, T. (2018). Mitochondria Affect Photosynthetic Electron Transport and Photosensitivity in a Green Alga. Plant Physiol. 176: 2305–2314.
Pubmed: Author and Title
Google Scholar: Author Only Title Only Author and Title

Munekage, Y., Hashimoto, M., Miyake, C., Tomizawa, K., Endo, T., Tasaka, M., and Shikanai, T. (2004). Cyclic electron flow around photosystem I is essential for photosynthesis. Nature 429: 579–82.
Pubmed: Author and Title
Google Scholar: Author Only Title Only Author and Title

Munekage, Y., Hojo, M., Meurer, J., Endo, T., Tasaka, M., and Shikanai, T. (2002). PGR5 is involved in cyclic electron flow around photosystem I and is essential for photoprotection in Arabidopsis. Cell 110: 361–71.
Pubmed: Author and Title
Google Scholar: Author Only Title Only Author and Title

Nawrocki, W.J., Bailleul, B., Cardol, P., Rappaport, F., Wollman, F.-A., and Joliot, P. (2019). Maximal cyclic electron flow rate is independent of PGRL1 in Chlamydomonas. Biochim. Biophys. acta. Bioenerg.
Pubmed: Author and Title
Google Scholar: Author Only Title Only Author and Title

Peltier, G., Aro, E.-M., and Shikanai, T. (2016). NDH-1 and NDH-2 Plastoquinone Reductases in Oxygenic Photosynthesis. Annu. Rev. Plant Biol. 67: 55–80.
Pubmed: Author and Title
Google Scholar: Author Only Title Only Author and Title

Peltier, G., Tolleter, D., Billon, E., and Cournac, L. (2010). Auxiliary electron transport pathways in chloroplasts of microalgae. Photosynth. Res. 106: 19–31.
Pubmed: Author and Title
Google Scholar: Author Only Title Only Author and Title

Shikanai, T. (2014). Central role of cyclic electron transport around photosystem I in the regulation of photosynthesis. Curr. Opin. Biotechnol. 26: 25–30.
Pubmed: Author and Title
Google Scholar: Author Only Title Only Author and Title

Shikanai, T. (2016). Regulatory network of proton motive force: contribution of cyclic electron transport around photosystem I. Photosynth. Res. 129: 1–8.
Pubmed: Author and Title
Google Scholar: Author Only Title Only Author and Title

Shikanai, T., Endo, T., Hashimoto, T., Yamada, Y., Asada, K., and Yokota, A. (1998). Directed disruption of the tobacco ndhB gene impairs cyclic electron flow around photosystem I. Proc. Natl. Acad. Sci. U. S. A. 95: 9705–9.
Pubmed: Author and Title
Google Scholar: Author Only Title Only Author and Title

Shikanai, T. and Yamamoto, H. (2017). Contribution of Cyclic and Pseudo-cyclic Electron Transport to the Formation of Proton Motive Force in Chloroplasts. Mol. Plant 10: 20–29.
Pubmed: Author and Title
Google Scholar: Author Only Title Only Author and Title

Shimakawa, G., Murakami, A., Niwa, K., Matsuda, Y., Wada, A., and Miyake, C. (2018). Comparative analysis of strategies to prepare electron sinks in aquatic photoautotrophs. Photosynth. Res.
Pubmed: Author and Title
Google Scholar: Author Only Title Only Author and Title

Storti, M., Alboresi, A., Gerotto, C., Aro, E.-M., Finazzi, G., and Morosinotto, T. (2019). Role of cyclic and pseudo-cyclic electron transport in response to dynamic light changes in Physcomitrella patens. Plant. Cell Environ. 42: 1590–1602.
Pubmed: Author and Title
Google Scholar: Author Only Title Only Author and Title

Suorsa, M., Järvi, S., Grieco, M., Nurmi, M., Pietrzykowska, M., Rantala, M., Kangasjärvi, S., Paakkarinen, V., Tikkanen, M., Jansson, S., and Aro, E.-M. (2012). PROTON GRADIENT REGULATION5 is essential for proper acclimation of Arabidopsis photosystem I to naturally and artificially fluctuating light conditions. Plant Cell 24: 2934–48.
Pubmed: Author and Title
Google Scholar: Author Only Title Only Author and Title

Terashima, I., Funayama, S., and Sonoike, K. (1994). The site of photoinhibition in leaves of Cucumis sativus L. at low

temperatures is photosystem I, not photosystem II. Planta 193.
Pubmed: Author and Title
Google Scholar: Author Only Title Only Author and Title

Tikkanen, M., Mekala, N.R., and Aro, E.-M. (2014). Photosystem II photoinhibition-repair cycle protects Photosystem I from irreversible damage. Biochim. Biophys. Acta 1837: 210–5.
Pubmed: Author and Title
Google Scholar: Author Only Title Only Author and Title

Tiwari, A., Mamedov, F., Grieco, M., Suorsa, M., Jajoo, A., Styring, S., Tikkanen, M., and Aro, E.-M. (2016). Photodamage of iron–sulphur clusters in photosystem I induces non-photochemical energy dissipation. Nat. Plants: 16035.
Pubmed: Author and Title
Google Scholar: Author Only Title Only Author and Title

Tjus, S.E., Møller, B.L., and Scheller, H. V (1998). Photosystem I is an early target of photoinhibition in barley illuminated at chilling temperatures. Plant Physiol. 116: 755–64.
Pubmed: Author and Title
Google Scholar: Author Only Title Only Author and Title

Wada, S., Yamamoto, H., Suzuki, Y., Yamori, W., Shikanai, T., and Makino, A. (2018). Flavodiiron Protein Substitutes for Cyclic Electron Flow without Competing CO2 Assimilation in Rice. Plant Physiol. 176: 1509–1518.
Pubmed: Author and Title
Google Scholar: Author Only Title Only Author and Title

Yamamoto, H., Takahashi, S., Badger, M.R., and Shikanai, T. (2016). Artificial remodelling of alternative electron flow by flavodiiron proteins in Arabidopsis. Nat. plants 2: 16012.
Pubmed: Author and Title
Google Scholar: Author Only Title Only Author and Title

Yamori, W. and Shikanai, T. (2016). Physiological Functions of Cyclic Electron Transport Around Photosystem I in Sustaining Photosynthesis and Plant Growth. Annu. Rev. Plant Biol. 67: 81–106.
Pubmed: Author and Title
Google Scholar: Author Only Title Only Author and Title

Yamori, W., Shikanai, T., and Makino, A. (2015). Photosystem I cyclic electron flow via chloroplast NADH dehydrogenase-like complex performs a physiological role for photosynthesis at low light. Sci. Rep. 5: 13908.
Pubmed: Author and Title
Google Scholar: Author Only Title Only Author and Title